THESIS

INSIGHTS INTO THE ORIGINS OF FUNCTIONAL MITRAL REGURGITATION AND DEVELOPMENT OF A CORRECTIVE EPICARDIAL DEVICE

Submitted by

Baptiste Gleyzolle

Department of Clinical Sciences

In partial fulfillment of the requirements

For the degree of Master of Science

Colorado State University

Fort Collins, Colorado

Summer 2010

COLORADO STATE UNIVERSITY

November 30th, 2009

WE HEREBY RECOMMEND THAT THE THESIS PREPARED UNDER OUR SUPERVISION BY BAPTISTE GLEYZOLLE ENTITLED INSIGHTS INTO THE ORIGINS OF FUNCTIONAL MITRAL REGURGITATION AND DEVELOPMENT OF A CORRECTIVE EPICARDIAL DEVICE BE ACCEPTED AS FULFILLING IN PART REQUIREMENTS FOR THE DEGREE OF MASTER OF SCIENCE.

Committee on Graduate work

E. Christopher Orton

Scott Earley

Susan P. James

Advisor: Eric Monnet

Department Head: D. Paul Lunn

ABSTRACT OF THESIS

INSIGHTS INTO THE ORIGINS OF FUNCTIONAL MITRAL REGURGITATION AND DEVELOPMENT OF A CORRECTIVE EPICARDIAL DEVICE

Functional mitral regurgitation (FMR) is a frequent complication of left ventricular remodeling and carries a significant adverse prognosis. While significant progress has recently been made in the understanding of the pathophysiology and treatment of this disease, failure to obtain acceptable outcomes is driving researchers and clinicians to investigate alternative approaches to the consensual treatments. A thorough understanding of the normal anatomy and physiology of the mitral valve is warranted to underline the pathophysiological mechanisms of left ventricular remodeling leading to functional mitral regurgitation. The accumulated experience with traditional techniques and the experimentation of emerging surgical procedures allowed us to identify strengths and points to be improved for each therapeutical approach. Based on this review, we defined the specifications of a new device designed to correct FMR.

In the first study we tried to develop an acute model of myocardial ischemia to induce mitral valve regurgitation in sheep. In six sheep, acute myocardial infarction was induced by ligation of the second and third obtuse marginal branches of the left circumflex coronary artery, defining an ischemic (IZ) and non ischemic (NZ) zone. Aortic and left ventricular pressures, left ventricular volumes, ECG, and segmental length of the IZ and NZ were recorded. Aortic blood flow was measured with an aortic flow probe in three sheep. Maximum elastance, dP/dt, tau, left ventricular and myocardial stiffness,

total mechanical energy (PVA), external work (Ew), contractile efficiency and the global and regional preload recruitable stroke work (PRSW and $rPRSW_X$) were calculated. Myocardial perfusion was calculated with injection of microspheres. Mitral regurgitant volume was calculated as the difference between the aortic and the left ventricular stroke volume. The data was compared between baseline, after five to ten minutes and one hour of ischemia. Myocardial blood flow decreased from 1.53 ± 0.81 mL/g/min to 0.37 ± 0.37 mL/g/min (p=0.022) in the IZ. Mitral regurgitation was not observed at any time point. Ischemia reduced PRSW from 60.7 ± 9.1 mmHg at baseline to 42.3 ± 4.3 mmHg and t+60 min (p=0.002), and $rPRSW_{IZ}$ from 96.2 ± 33.9 $mmHg.L.m^{-1}$ at baseline to 59.2 ± 28.6 $mmHg.L.m^{-1}$ at t+5-10 min (p=0.026) and 63.7 ± 25.7 $mmHg.L.m^{-1}$ at t+60 min (p=0.032). PVA decreased from 6260 ± 1387 mmHg.L at baseline to 4149 ± 1299 mmHg.L at t+5-10 min (p=0.019) and 4368 ± 1632 mmHg.L at t+60 min (p<0.001). Ew decreased from 3877 ± 1287 mmHg.L at baseline to 2334 ± 872 mmHg.L at t+5-10 min (p=0.037) and 2507 ± 883 mmHg.L (p=0.013) at t+60 min. Myocardial stiffness of the IZ decreased from 2.63 ± 1.23 mm^{-1} at baseline to 0.94 ± 0.57 mm^{-1} at t+5-10 min (p=0.014) before an increase to 3.56 ± 0.57 mm^{-1} at t + 60 min (p=0.033). In conclusion, acute occlusion of OM2 and OM3 did not induce acute functional mitral valve regurgitation. It did however, induce early systolic and diastolic regional dysfunction. The non-ischemic myocardium did not compensate for the left ventricular remodeling.

In the second study, we used acute aortic banding to induce mitral valve regurgitation. This was done to assess the effects of an epicardial device designed to reposition the papillary muscles on FMR, considering that left ventricular remodeling with tethering of the papillary muscle is the most important factor leading to FMR. In seven sheep, aortic, left ventricular and atrial pressures, left ventricular volumes, aortic blood flow, mitral annulus diameter and ECG were recorded. Acute FMR was induced by aortic

banding. Left ventricular end diastolic and end systolic volume, stroke volume, the constant of passive left ventricular stiffness and Tau were measured. Mitral regurgitant flow was calculated from the difference between aortic stroke volume and left ventricular stroke volume. Application of an epicardial device reduced FMR from 14.4 ± 5.4 to 7.7 ± 5.2 mL (p=0.001) without decreasing mitral annulus diameter in diastole (p=0.075) and systole (p=0.080). Left ventricular end diastolic volume decreased from 241.5 ± 52.5 to 227.6 ± 46.5 mL (p=0.044). Passive left ventricular stiffness increased from 0.92 ± 0.5 to 1.18 ± 0.59 mL^{-1} (p=0.044). Other parameters of diastolic dysfunction were not affected by the device. In conclusion, acute FMR was decreased by the application of an epicardial device. Diastolic function was not adversely affected by the device. Most likely, correction of FMR by the epicardial device was achieved by repositioning of the papillary muscles. The epicardial device was not in contact with blood and did not require cardiopulmonary bypass.

Baptiste Gleyzolle
Clinical Sciences
Colorado State University
Fort Collins, CO 80523
Summer 2010

ACKNOWLEDGEMENTS

From the formative stages of this thesis, to the final draft, I owe an immense debt of gratitude to my supervisor, Eric Monnet, whose encouragement and guidance enabled me to develop an understanding and basic knowledge of the cardiovascular physiology. My experience in the United States has broadened my mind more than I ever could have imagined. This would not have been possible without your constant help and support. Thank you.

I would like to express my gratitude and respect to the members of my committee for their comments, suggestions and criticisms that played a major role in the improvement of this work. Thank you for your support.

DEDICATION

I would like to dedicate this thesis to my brother, my parents and grand-mother who have always been here for me through the good and bad times. Their unconditional support gave me the motivation to never give up.

To Maud, Perrine and Victor, being here for me is something I will never forget. You know the special place you hold in my heart. Thank you.

To Brad, Claire and Asher. Words wouldn't be strong enough to express what I feel for you guys.

To Colin, Мы останемся друзьями надолго.

To Lisi, who stayed by my side despite the distance. I wish you the happiest life.

To my close friends in the Fort. Please know that you can count on me, as much as you were there for me.

To the professors of the VTH who helped me through my internship and who played an active role in my clinical mentorship, I thank you.

"Impose ta chance, serre ton bonheur et vas vers ton risque. A te regarder, ils s'habitueront." Rene Char.

TABLE OF CONTENTS

LISTE OF TABLES

LIST OF FIGURES

Chapter I

Introduction

Cardiovascular diseases has become over the last 50 years the number one cause of death and hospitalization in the United States as well as other developed countries. The population pays a significant price for these pathologic conditions, in part from the mortality but also due to the cost associated with treatment and socioeconomics.[1] Among cardiopathies, coronary artery disease is from far the most common and is often associated with functional mitral regurgitation (FMR).[1-5] Secondary to left ventricular remodeling, FMR is a challenge for cardiovascular surgeons. Indeed, a poor long term prognosis and increased morbidity is associated with this condition despite the advances made in cardiac surgery.[3, 6]

After an anatomical review of the mitral apparatus focusing on the aspects playing a crucial role in the genesis of FMR, the second chapter will further develop the pathophysiologic events leading to FMR. The third chapter will review the current available therapeutic options, their clinical implications and the future directions to be followed in hopes of obtaining more successful clinical outcomes.

Chapter II

Natural history of the mitral valve

The understanding of the normal mitral valve physiology relies on the knowledge of its anatomy and spacial organization.

1. Using the ovine model as a comparative study

The ovine model is recognized as a valuable tool for studying mitral valve function, particularly ischemic heart diseases. Its mitral physiology is thought to be similar to the human being, however, some slight anatomical singularities distinguish sheep from human hearts. In the sheep, the mitral leaflets attach to atrial muscle rather than to the ventricle, the relative length of free papillary muscle is greater[7] and the coronary anatomy is highly reproducible between individuals,[8, 9] as compared to the human.

Those specificities do not seem to affect the pathophysiology of mitral valve diseases, and most of the structure and function of the mitral apparatus is highly comparable between sheep and humans. Hence, from now in this study, no differences will be asumed between human and the ovine model, unless specified.

2. Anatomical considerations

i. Structural components

The valvular complex comprises the annulus, the valve leaflets and the tensor apparatus formed by the cordae and the papillary muscles.

a. Annulus

The annulus is the fibrous like structure supporting the leaflets and demarcating the orifice between the left atrium and the left ventricle. This orifice is D shaped with the straight border in fibrous continuity with the aortic valve. Considering this asymmetry, two dimensions of the annulus are described: the septo-lateral axis is perpendicular to the valves and represents the short dimension, as opposed to the anterio-posterior axis. The fibrous tissue is organized in discontinued sheet like fibrous extensions of the aortoventricular membrane that expends around the subvalvular region. An extensive variability of the fibrous organization of the annulus has been described,[10] with a lack of continuity observed in the lateral side of the annulus. Consequently, this weakened side tends to dilate first secondary to various cardiomyopathies.[10]

In vivo, the annulus is not entirely in the same plane, and is echographically described as «saddle shaped», forming a hyperbolic paraboloid with the lowest points at the level of the leaflet commissures (Figure 2.1).[11, 12] This curvature is exacerbated during systole, reducing the stress of the mitral valve components.[13]

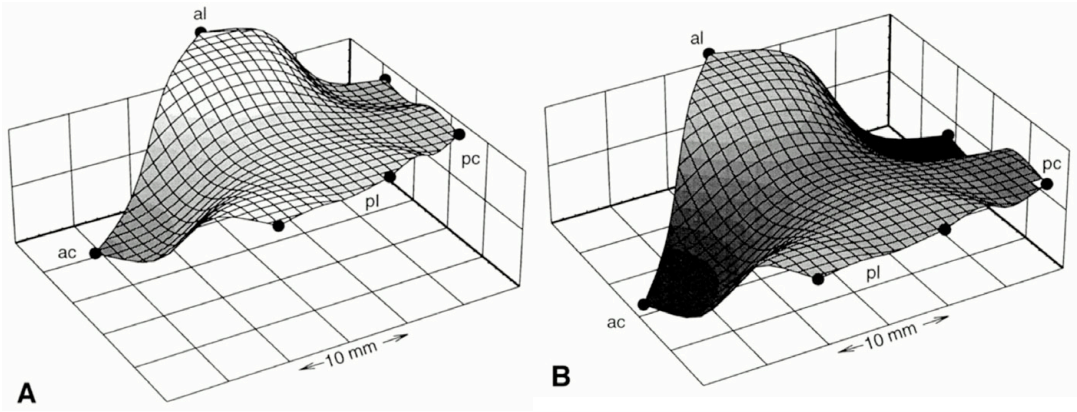

Figure 2.1: Schematic representation of the mitral annulus shape at end-diastole (A) and end-systole (B). ac: anterior commissure, pc: posterior commissure, al: aortic commissure hinge, pl: mural commissure hinge. Gorman III et al. 1996

b. Valve leaflets

Two notably different leaflets compose the mitral valve. The aortic or septal leaflet, smooth and semicircular, occupy approximately one third of the circumference of the annulus and are in fibrous continuity with the aortic valve. The mural leaflet, long and narrow, occupies the remainder of the circumference and is usually partially divided in three scallops by two clefts.

The leaflets have a fibrous skeleton (fibrosa) covered on their atrial side by a myxomatous connective tissue (spongiosa). Atrial and ventricular endocardium respectively lie on each side of the leaflets. The total mitral leaflet area is 1.5 to 2 times the annular area.[14] The difference between the leaflet and the annular area when the valve is closed is to be found on the coaptation surface, i.e. The surface of leaflet apposition. This apparent excess of leaflet surface is defined as the functional reserve of the mitral valve and allows a tight coaptation under a broad range of hemodynamic conditions.

When seen in transection, two zones can be distinguished in the aortic leaflet and three in the mural leaflet. Near the free edges of both leaflets, the atrial surface is irregular with nodular thickening. This is the thickest part of both valves, the tendinous cords attaching to this rough zone. Broadest at the lowest portions of the leaflets, this zone tends to taper towards the commissures.[10, 14-16] Distal to this area in regard to the free edges, the leaflets possess a clear zone devoid of cordal attachments. The basal zone is only found on the ventricular side of the mural leaflet and corresponds to the area of attachment of the basal cords.[10, 14-16]

c. Papillary muscles and cordae

Two groups of papillary muscles are classically described in the left ventricle. The posteromedial group lies near the posterior attachment of the left ventricular free wall and the interventricular septum, while the anterolateral group lies on the anterolateral left ventricular free wall.

As functional units, the papillary muscles include a portion of the left ventricular wall, usually the apical and middle thirds of its width.[15] While the spacial organization of the numerous muscular bundles forming the base of the papillary muscles is highly variable, the distal tips supporting the cordae form muscular columns with precise spacial positioning which plays a critical role in the distribution of forces and proper closure of the mitral valve.[14, 17, 18]

The tendinous cords represent a complex rope like structure composed of highly bound collagen linking the ventricular free edges of the leaflets to the papillary muscles. The basal cords attach the leaflets directly to the posteroinferior left ventricular wall, while the cords arising from the apices of the papillary muscle attach to both the aortic and lateral leaflets.[14, 15] Several classifications have been proposed in relation to the anatomical localization, structure and function of the cords[14, 15] .

The first order cords (commissural or marginal) insert near the edges of the leaflets. They are numerous, thin, and form a meshwork close to their attachment to the leaflets (Figure 2.2). Second order cords insert on the rough zone of the leaflets. The cords in the rough zone typically originate as a single cords from the tip of the papillary muscles and split into three cords. Among the cords of the septal leaflet, two are the largest and the strongest. They are named strut cords and arise from both tips of the papillary muscles. They are though to support the maximum force. Basal cords originate

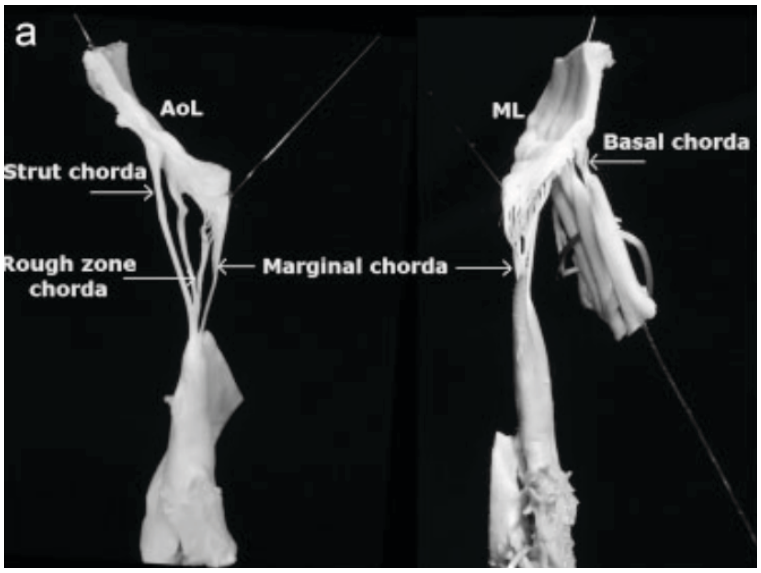

Figure 2.2: Tendinous cords of the mitral valve. Anatomical preparation showing the distribution of the cordal support of the aortic leaflet (AoL) and mural leaflet (ML). Muresian 2009

directly from the left ventricular wall or the trabecular region of the posterior papillary muscle and are linked to the atrial myocardium (basal portion) of the mural leaflet.[14-16]

ii. Vasculature of the mitral valvular complex

Coronary arteries in the subepicardial fatty tissue give birth to finer perpendicular arborizations (class A) perfusing the middle and outer third of the myocardium[19] (figure 2.3). The larger arborizations (class B) divide less frequently and terminate as an anastomotic meshwork perfusing the inner third of the myocardium, the endocardium and the papillary muscles. Each papillary muscle is vascularized with several of these branches.[14, 19] The trabeculae bridging the papillary muscles to the left ventricle often carry those segmental blood vessels.[19]

Most of the time, the anterior papillary muscle is perfused by both the first obtuse marginal branch of the left circumflex coronary artery and the first diagonal branch of the

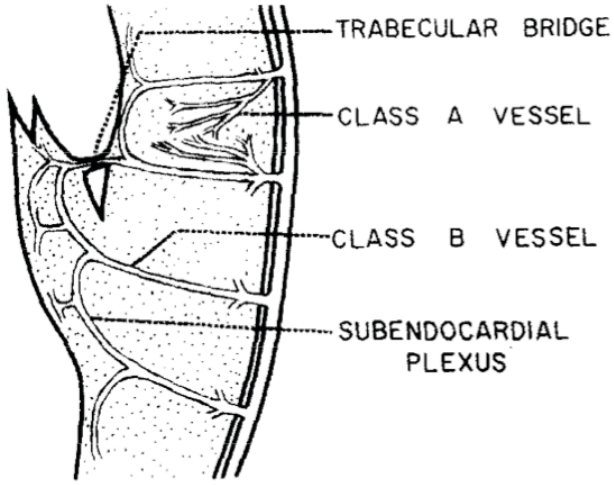

Figure 2.3: Schematic representation of the blood supply of the normal papillary muscle. Estes et al. 1966

left anterior descending artery.[20] In the human being, the vascularization of the inferoposterior left ventricular wall and the posterior papillary muscle is variable. In the right dominant system, this zone is perfused mostly by the distal right circumflex coronary artery and in some cases the third obtuse marginal branch of the left circumflex coronary artery.[14, 19, 20] In the left dominant system however, the posterior papillary muscle and the inferoposterior region of the left ventricular wall is irrigated by the second and third obtuse marginal branch of the left circumflex coronary artery.[14, 19, 20]

In the sheep, the coronary vascularization is comparable to a left dominant system. The coronary pattern is very constant between individuals.[8]

3. Mitral valve function during the cardiac cycle

The normal closure starts in early systole with a sphincteric mechanism of the annulus elevating the aortic leaflet towards the mural one.[21] Left ventricular contraction subsequently increases the pressure gradient between the ventricle and the atrium, eventually bringing the leaflets towards the plane of the annulus according to the coapting force.[18] An adequate inter-scallop coaptation appears to be of equal importance

to the inter-leaflet coaptation for the valve competence.[22] During peak systolic pressure, most of the cordae are aligned in the same plane, which is the plane of the coaptation surface, roughly in the atrioventricular axis.[18, 23] The increasing stress is progressively supported by a growing number of increasingly thick chords that can share the stress between them according to their thickness (Figure 2.4).[23]

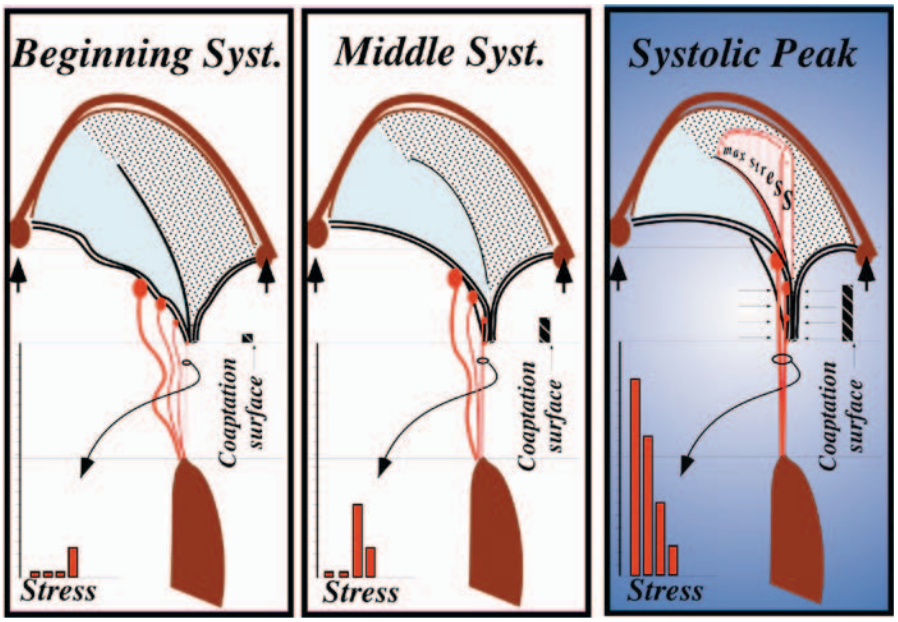

Figure 2.4: Schematic representation of the mitral valve during systole. During the systolic peak under maximum stress, all the chordea are in the same plane. Nazari et al. 2000

The rough zone acts in functional continuity with the cordea, distributing equally the amount of tethering force on the leaflets.[18, 23] Hence, the leaflets normally coapt by apposition of the rough zones in a plane apical to the annulus, the cords and papillary muscles defining a tenting area and a tenting volume. The spatial positioning of the papillary muscles plays a critical role in the coaptation of the valve leaflets since they support the majority of the cordae, and are responsible for the adequate distribution of the tethering forces.[18] During the cardiac cycle, the papillary muscle tips keep a constant distance relative to the annulus.[21] It is now recognized that the papillary muscles function

as a separate unit from the left ventricle. They act as shock absorbers to compensate for the changes in left ventricular geometry, maintaining a constant tip to annulus length.[24]

Appropriate function of the mitral valve is accomplished by the fine organization and function of all its structural components. Any pathology leading to the modification of one or several of those parameters can induce dramatic dysfunction of the mitral valve.

Chapter III
Pathophysiology of functional mitral valve regurgitation

Primary mitral regurgitation is a condition in which pathology of the mitral apparatus has caused the mitral valve to leak. In contrast, functional mitral regurgitation is induced by pathology of the left ventricle causing an otherwise normal mitral valve to be incompetent.

1. Etiologies of FMR

By definition, FMR is seen when the mitral valvular complex is modified enough to perturb the forces leading to the natural function of the leaflets. This condition happens secondary to left ventricular remodeling: enlargement of the left ventricle with tethering of the cordea and augmentation of the interpapillary distance, annular dilatation, ventricular dysfunction and asynchrony of the papillary muscles contractility. Classically, FMR is characterized as ischemic or non-ischemic. With non-ischemic causes of FMR, the left ventricular dysfunction is global. Idiopathic dilated cardiomyopathy or dilated cardiomyopathy secondary to aortic stenosis are the most common causes of non-ischemic FMR. In contrast, left ventricular infarction due to coronary disease causes regional wall disfunction and may lead to ischemic FMR if the left ventricular dilatation is severe enough.

2. Effect of left ventricular remodeling and papillary muscle tethering

Otsuji et al.[25] showed that alteration of the tethering forces on the mitral valve induces MR rather than contractile dysfunction. They pharmacologically induced global left ventricular dysfunction limiting left ventricular dilatation with a pericardial restraint.Only trace MR was observed, while FMR developed immediately after removal of the constraint, illustrating that left ventricular dilatation was a prerequisite to FMR.[25] They found that tethering length from the papillary tips to the anterior annulus was the only independent predictor of MR.[25]

In addition, isolated papillary muscle dysfunction without left ventricular dilatation does not induce MR while a preserved papillary muscle function with left ventricular remodeling does not prevent MR.[26] In this condition, ischemic MR can paradoxically be reduced inducing papillary muscle ischemia.[27] Papillary muscle dysfunction decreased

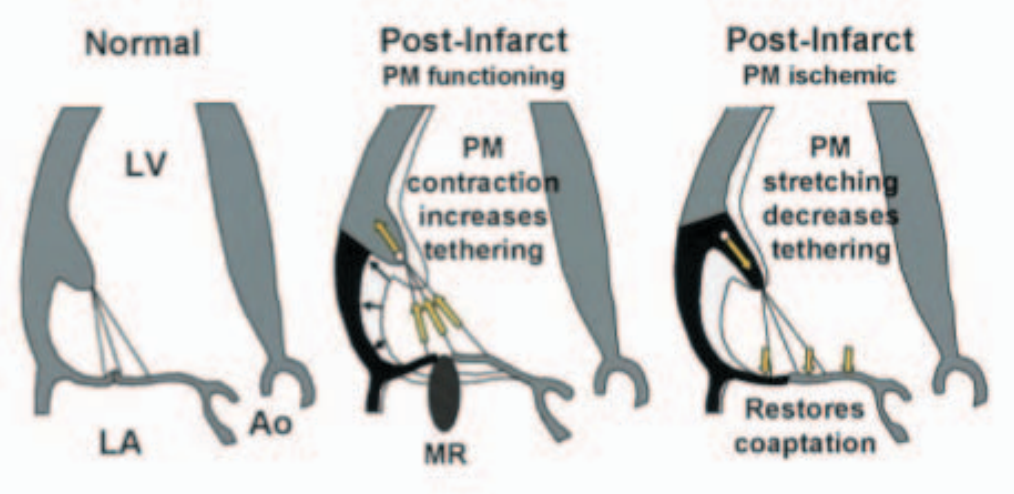

Figure 3.1: How papillary muscle (PM) dysfunction can decrease mitral regurgitation (MR). Left: schematic view of the left ventricle and mitral valve. LV: left ventricle, LA: left atrium, Ao: aorta. Center: inferobasal infarction with PM still functioning causing MR with leaflet tethering and tenting. Right: extension of ischemia to papillary muscle causes its dysfunction and paradoxical decrease in MR *via* decreased tethering. Messas et al. 2001

leaflet tethering due to their elongation, improving coaptation of the mitral valve (figure 3.1). In contrast, chronic injection of ethanol in papillary muscles causes scarring and retraction induced MR.[28]

Those observations emphasize the importance of papillary muscle displacement and tethering forces on the genesis of mitral regurgitation.

Although simultaneous displacement of both papillary muscles can lead to MR, the posterolateral papillary muscle seem to play a more important role for the apparition of MR. Hence, Kumanohoso et al.[5] studied the incidence of MR in a population of patients with no prior myocardial infarction. The higher incidence and greater severity of MR was observed in patients with inferior basal infarction. This observation was correlated with more severe geometric changes involving the posterolateral papillary muscle.[5] This observation was also described by Timek et al.[29] who investigated different locations of left ventricular ischemia. MR was induced by proximal left circumflex coronary artery occlusion but not during left anterior descending or posterior left circumflex coronary artery occlusion. Posterolateral ischemia increased tethering of the papillary muscles, delayed valve closure in early systole and caused dilatation of the annulus.[29]

3. Altered annulus and leaflet function during MR

i. Annulus changes contributing to MR genesis

a. Loss of contractility

During FMR the dynamic behavior of the annulus is impaired.[30] While a normal annulus exacerbates its saddle shape during systole, this sphincteric mechanism is decreased during ischemia. The systolic increase in average change in annular height to commissural width ratio (AHCWR) is then lost during ischemic mitral regurgitation.[30] As

we saw above, the saddle shape of the annulus during systole is crucial to minimize the stress of the leaflets.[13] Loss of saddle shape is a factor contributing to leaflet tenting and tethering during FMR. This functional disarrangement are associated in addition with some degree of annular dilatation.

b. Annular dilatation

In acute ischemic mitral regurgitation or in chronic FMR an increase in septo-lateral dimension of the annulus is often implicated in leaflet malcoaptation.[31, 32] More specifically, the right lateral annulus moves laterally, respectively away from the anterior papillary muscle.[22] This asymmetrical dilatation is the origin of interscallop malcoaptation, thought to be important in the genesis of ischemic MR.[22] Mitral regurgitation however, is not associated with the commissure to commissure dimension of the annulus.[33] In dilated cardiomyopathy, for virtually the same grade of MR, the annulus is more dilated with a symmetrical deformation compared to an ischemic disease.[12] Park et al.[34] correlated the severity of MR to the mitral annular area in a recent study including a population of patients with advanced dilated cardiomyopathy. This observation is controversial since some authors describe that isolated increase in annulus diameter without increase in tethering length is not associated with MR.[35, 36]

Hence, annulus changes alone do not create MR but as part of the unifying principle of mitral valve function, remodeling of the annulus plays a direct role in leaflet geometry and motion, impaired during FMR.

ii. Leaflets coaptation defines mitral competence

a. Effects of the left ventricular remodeling on the leaflets geometry

As described above, the leaflet motion and stabilization is intimately associated with the spacial organization of the cordae and papillary muscles. Glasson et al.[31]

studied lealfet motion and mitral valve geometry during acute anterobasal left ventricular ischemia. They observed a posterolateral displacement of the posterior papillary muscle during end-diastole as well as a posterior mitral annulus enlargement. Interestingly, leaflet malcoaptation was present in early systole but the valve became competent during mid-systole. They termed this abnormal motion «loitering».[31] They noted however that the coaptation plane remained similar to that of the control group. Using a theoretical model of the tensor apparatus during systolic stress, Nazari et al.[23] demonstrated that dilatation of the annulus and leaflet tethering disarranged the chordal apparatus radially: the coaptation plane surface is deviated relatively to the second order chordae, causing the chordae closer to the free margin to be overloaded in early systole.[23] At peak systolic stress, the mitral leaflets become tented as maximum load is applied on the second order cords.[12, 37] This tenting volume has been correlated with the degree of MR,[37] and is now considered a reliable index for the quantification of subvalvular remodeling.[38]

b. Insights into the dynamic lesion of mitral leaflets during FMR

This study hence introduces the idea of the dynamic balance of the forces involved in mitral function and the impact of geometrical disarrangement. Nielsen et al.[18] studied in vitro the mitral coaptation geometry isolating the chordal force components (Figure 3.2).

Mitral valve competence is guaranteed by the force equilibrium resulting in the chordal tethering force component F_T and the chordal coapting force component F_C. While F_T is determined by the spacial relationship of the papillary muscles, F_C is determined by the forces applied by the transmitral pressure difference acting on the leaflet surface. In normal conditions, each force component of the cordae is uniaxially parallel and opposed resulting in a null balance equilibrium.[18, 39] Posterolateral

displacement of the papillary muscles increased the tethering force significantly,[18, 40] however, the coaptation force increased for the aortic leaflet and decreased for the mural leaflet, reducing considerably its occlusional area.[18] This caused an asymmetrical coaptation pattern shifted posterolaterally which was also described clinically.[41]

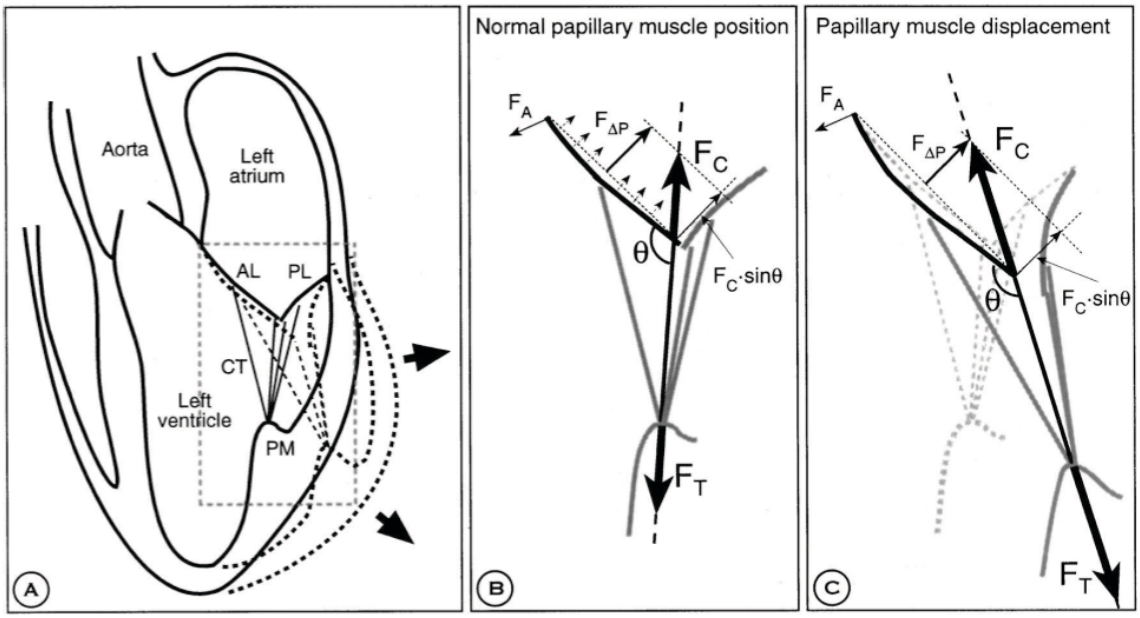

Leaflet «loitering»[31] and mitral regurgitant flow is then observed in early and late systole when the coaptation force is lower than the tethering force applied on the mural leaflet.[42] During the peak systolic stress, the sum of coaptation forces overcomes the tethering forces and the valve becomes competent, unless the annular dilatation or the tenting is too severe. If the systolic function is impaired, one might think that the left ventricle may not develop an adequate transmitral pressure gradient, diminishing the coaptation forces, and perhaps worsening the mitral insufficiency.

c. Compensatory mechanisms for FMR

Since the mitral valve leaflet can acutely and reversibly elongate up to 15% under physiological conditions,[43] it is reasonable to think that mitral valve leaflets may compensate for the increased stress due to left ventricular remodeling by enlargement. Stiffening of the leaflets with increased collagen concentration has been reported in

severe heart failure patients,[44] and a recent study showed that mitral valve leaflet surface was 35% greater in patients with chronically tethered leaflets compared to normal control subjects.[45] They hypothesized that significant MR may develop or worsen in the face of chronic leaflet tethering due to insufficient leaflet adaptation. The variability of compensatory response may explain the heterogeneity of FMR severity seen among patients.[45] The question wether this leaflet adaptation to increased tethering is a passive stretch or involves active histologic changes has been investigated recently by Dal-Bianco et al.[46] In a model of mitral leaflet tethering without MR nor ischemia, they observed increased leaflet area and thickness. Interstitial matrix was produced by activated mesenchymal and endothelium cells.[46] To avoid confounding factors, they chose a model with no MR since turbulent flow induces focal leaflet thickening and may further signal remodeling.[47, 48] For a similar reason, an ischemic model could have interfered since the infarcted myocardium and its borderzone region may stimulate leaflet growth and collagen production.[48]

Hence, modified mechanical stresses induced by left ventricular remodeling is promote an active compensatory phenomenon which may become maladaptative with chronicity.[47]

Tosummarize, functional mitral regurgitation is a complex pathology secondary to left ventricular remodeling. Many structural and functional components play a role in its genesis and evolution, including the compensatory attempts. Papillary muscle tethering of the mitral valve appears to be the most important factor leading to MR. It is crucial to understand the mechanisms involved with this condition to find the most appropriate therapeutic options, today limited in their long term results.

Chapter IV

Therapeutic options for a dynamic structural disease

1. Prognosis of patients diagnosed with FMR

FMR occurs in roughly 50% of patients with congestive heart failure[49] and 20% to 25% of patients followed up after myocardial infarction.[2-5] Among those patients, FMR carries an adverse prognosis with a graded relationship between severity of mitral regurgitation and survival (Figure 4.1 and 4.2).[3, 6]

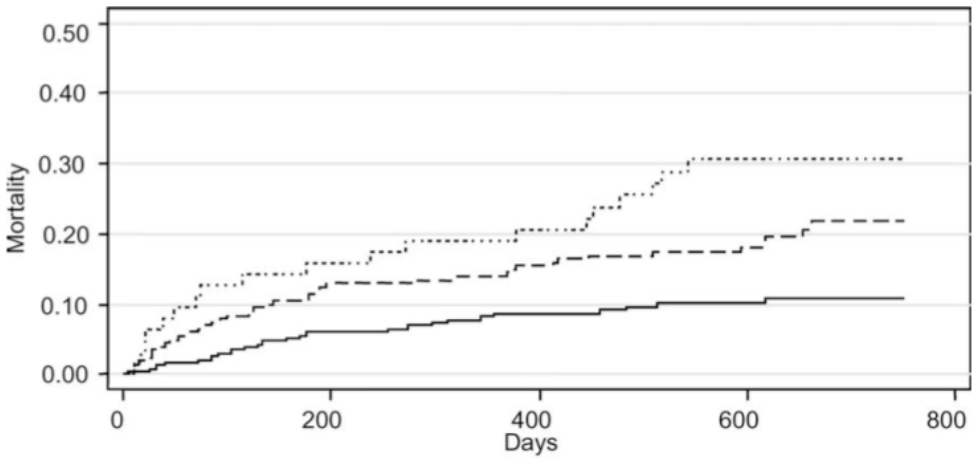

Figure 4.2: Kaplan-Meier survival curves divided according to the severity of MR. Solid line: no MR, dashed line: mild MR, dotted line: moderate to severe MR. The patients were only under medical treatment. Amigoni et al. 2007

Furthermore worsening of MR between baseline and one month is associated with increased adverse outcomes.[6]

Although demonstrated to be actively associated with worsening of left ventricular remodeling, survival and morbidity, correction of FMR is still hotly debated.[50] The debate takes its origins in the facts that the actual available therapeutic options do not provide satisfying results on a mid to long term and they are inherently associated with surgical risks and morbidity.

2. Treatment of FMR

Like any other pathologic process, prevention, limitation of the risks factors and early detection and treatment of FMR are of crucial importance. For dilated cardiomyopathy patients, this means early medical management to limit left ventricular remodeling, while for patients undergoing left ventricular infarction, limiting the infarct size and extension is the aim. If MR develops or worsens despite preventive or first line measures, two axes of treatment can be envisioned: restoring leaflet coaptation with valvuloplasty or annuloplasty procedures or restoring subvalvular geometry with ventriculoplasty techniques or with procedures modifying papillary muscles positioning.

Each technique currently described has advantages and drawbacks. Through a brief review of the therapeutic options used or in development, we will try to define specifications for the development of a new device able to correct FMR.

i. Restoring leaflet coaptation

To date, the standard of care to treat FMR is based on annuloplasty techniques. The rationale is that restoring coaptation addressing the annular geometry, correction MR at the time of surgery may become permanent and sufficient to stabilize the left ventricular remodeling and prevent heart failure events.

Because of the work of Kay et al.[51] demonstrating the better short and long term outcome, mitral repair has became the preferred method against mitral replacement for

treatment of FMR. Gillinov et al.[52] confirmed this evaluation, however they found that in high-risk sick patients, the survival was equivalent.

The superiority of repair over replacement is demonstrated by the fact that the surgical time is lower, there are no potential complications associated with prosthetic deterioration or malfunction, and most importantly the subvalvular apparatus is spared. Repair techniques result then in some degree of left ventricular function improvement due to the maintenance of the ventricular to valvular mechanical relationship.

a. Undersized annuloplasty

Undersized annuloplasty has become the treatment of choice of FMR following the work of Bolling et al.[53], and is sometimes associated with CABG. The goals of this procedure are to decrease the annular septo-lateral dimension to increase leaflet coaptation. Many types of prosthetic rings are available: complete, incomplete, rigid, flexible, symmetrical or not. Several authors argue in the literature the merits of one type of implant versus another, but no definite advantage has been shown, at the exception of pericardial bands that carry a worse long term prognosis.[54]

Early results for mitral annuloplasty were encouraging with a relatively low perioperative mortality rate[55] and residual MR (Figure 4.3).[54, 56] The clinical benefits of this technique are still strongly debated. Despite these interesting early results, a disappointing high rate of MR recurrence is observed generally a few months post correction, ranging from 17 to 35 percent according the studies.[54, 56-58] To obtain conclusive results concerning the survival rate, control groups have to be chosen with caution with an unbiased population. Two large retrospective analysis with rigorous entry criteria with ischemic MR compared the five years survival of patients who underwent undersized annuloplasty and revascularization to a group of patients who had revascularization only.[59, 60] No survival benefit could be attributed to valve intervention

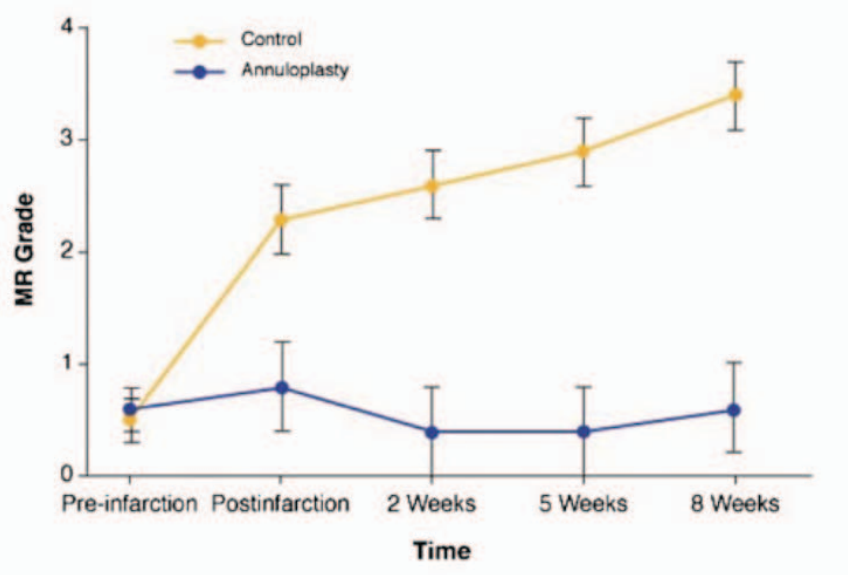

Figure 4.3: Mitral regurgitation control versus annuloplasty. Gorman III, 2006

compared to control, in each study the five year survival being 50 percent or less.[59, 60] Mitral valve repair did however decrease the incidence of symptomatic heart failure.[59]

Undersized annuloplasty improve mitral leaflet coaptation but does not address subvalvular changes (Figure 4.4). Left ventricular remodeling is the primary factor

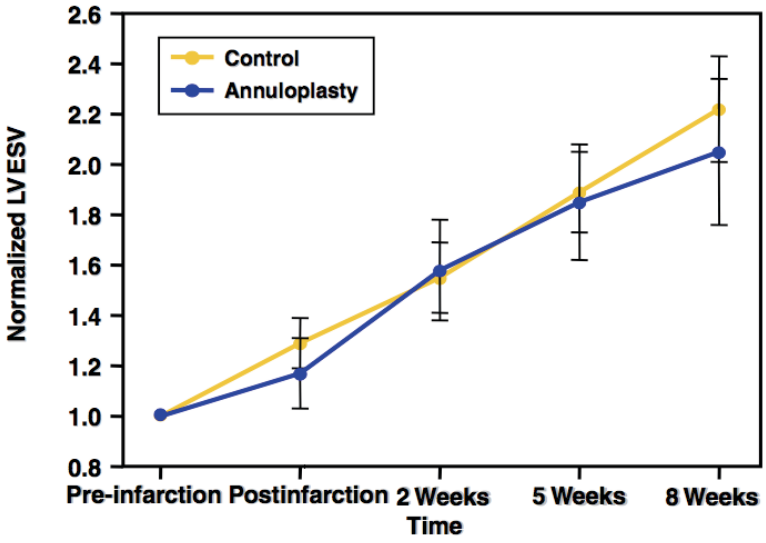

Figure 4.4: Left ventricular end-systolic volume, control versus annuloplasty group. Guy et al. 2002

contributing to alteration of the valvular complex geometry and is not addressed by undersized annuloplasty.

Guy et al.[61] and Enomoto et al.[62] prophylactically placed annuloplasty rings before myocardial ischemia in sheep. Although they did not see significant MR eight weeks post infarction, left ventricular remodeling was comparable with the control groups (Figure 4.4). Hung et al. Also recognized this phenomenon of left ventricular remodeling clinically.[63] Those observations led the clinicians to investigate the potential predicting factors of MR recurrence after annuloplasty. In a very recent study, Onorati et al.[64] found that recurrence of ischemic MR following undersized annuloplasty correlated with the

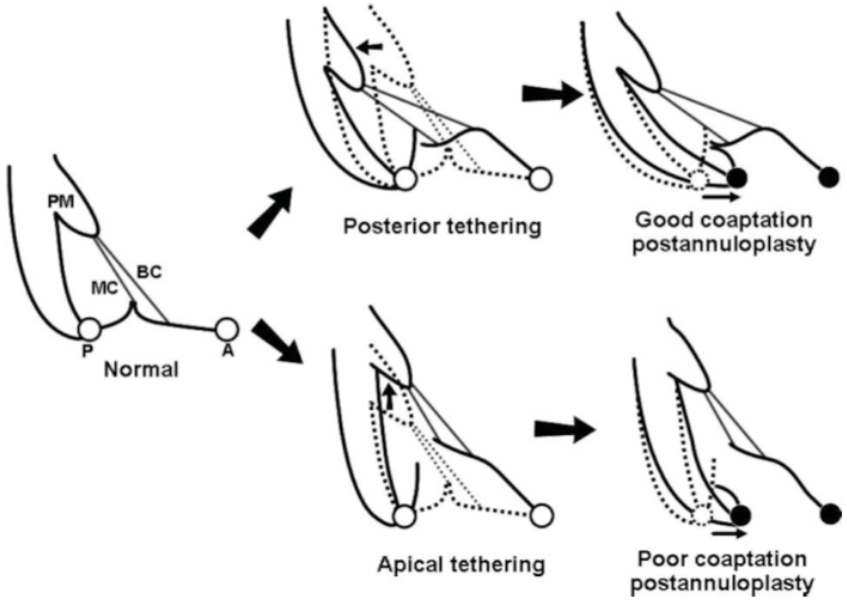

Figure 4.5: Schematic representation of the mitral valve and proposed mechanisms for apical and posterior tethering. A: aortic leaflet, BC: second order chordae, MC: marginal chordae, P: mural leaflet, PM: papillary muscle. Lee et al. 2009

signs of absence of reverse ventricular remodeling. Tethering of the mitral leaflets and left ventricular dilatation tended to increase the risk of recurrence.[64] Lee et al.[65] demonstrated that apical tethering of the aortic leaflet is a major cause of annuloplasty

failure (Figure 4.5). Hence, undersized annuloplasty does provide some benefits in some patients but the risks associated with the procedure (risk of repair failure and poor long term survival rate) justify investigation in to alternative procedures.

b. Valvuloplasty techniques

Edge-to-edge techniques

Alfieri et al.[66] originally developed edge-to-edge suture techniques for various mitral valve diseases. The technique is relatively simple and fast to execute (Figure 4.6). A ring annuloplasty has to be performed concomitantly otherwise the results are disappointing in the long term.[67] Like annuloplasty alone, more than 30 percent of patients with ischemic cardiomyopathy undergoing this procedure have a moderate to

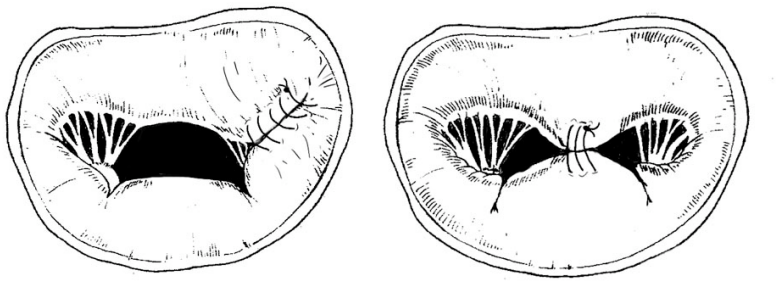

Figure 4.6: Edge-to-edge suture. Left: commissural suture, right: double-orifice suture. De Bonis 2002

severe recurrent MR at one year post mitral valve repair.[68] The authors concluded that this subcategory of patients may not be optimal candidates for this technique.

A percutaneous variant of the edge-to-edge repair has been developed in a porcine model using catheter delivered clips, but the success remains dependent on an additional annuloplasty intervention.[69]

Posterior mitral valve restoration

Fundaro et al.[70] introduced a technique for the correction of asymmetrical annulus dilatation encountered during ischemic cardiomyopahies. They aimed to

decrease leaflet tethering *via* reduction of annular septo-lateral dimension and approximate the papillary muscles with a reconstruction technique.

c. Percutaneous annular reduction

A variety of devices have been developed for percutaneous annuloplasty techniques. They are implanted in or in proximity of the coronary sinus. Representative examples are the Percutaneous Transvenous Mitral Annuloplasty (PTMA) formed of three stainless steel rods, the CARILLON Mitral Contour System, an anchored nitinol bridge or the Percutaneous Septal Sinus Shortening (PS3), an anchored stent.[71]

Several drawbacks to those techniques will need to be addressed before use in the clinical setting. The first problem arises from the anatomy of the coronary sinus in the human being. Maselli et al.[72] reviewed 61 anatomical preparation from excised human hearts and showed that a large number of specimen had several large branches of the main circumflex coronary artery that were running between the anterior interventricular vein, the coronary sinus and the annulus. The risk of compressing a coronary artery with a percutaneous device has to be taken in to consideration.[72] Finally, the devices placed within the coronary artery may carry a thrombogenic risk.

Relative disappointing long term results of valvular procedures led the clinicians and investigators to focus more on the correction of the subvalvular apparatus geometry, either with a single intervention or in conjunction with an annuloplasty technique.

ii. Correction of the chordal-valvular apparatus tethering

As we saw above, most of the complications and failure of the interventions used to date are reasonably related to the fact that none are able to stabilize or reverse left ventricular remodeling. With this paragraph we will review the described techniques that aim at restoring physiological balance to the subvalvular apparatus.

a. Procedures for the chordal apparatus

Second-order chordal cutting

Considering the fact that tethering of the aortic mitral leaflet is a major player for the genesis and that second-order chordae are responsible of this tethering, Messas et al.[73, 74] developed the technique of second-order chordal cutting. This operation does not reposition the papillary muscle in their physiologic position, however relief of the tethering allows a new mechanical balance of the chordal-valvular apparatus (Figure 4.7). In an animal model, Messas et al.[75] demonstrated that chordal cutting did not have

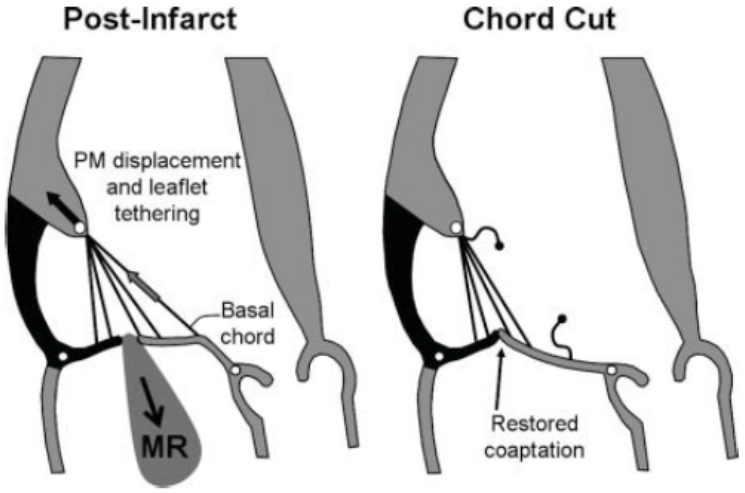

Figure 4.7: Chordal cutting. Left: papillary muscle displacement secondary to inferobasal infarction tethers the aortic leaflet, right: second-order chordae cutting restores leaflet coaptation. PM: papillary muscle, MR: mitral regurgitation. Levine et al. 2005

adverse effect on left ventricular dynamics and energetics in response to concerns regarding altered leaflet motion and left ventricular stability.[76, 77] Indeed, a retrospective study comparing patients with ischemic MR who underwent undersized annuloplasty or chordal cutting showed promising two-year follow-up results for the chordal cutting group.[78] Although no significant differences were found in survival rate or factors predictive of survival between groups, they did find that chordal cutting decreased the

recurrence rate for MR from 37 percent to 15 percent.[78] Interestingly atrial fibrillation was significantly higher in the chordal cutting group compared to the control. This observation should not be observed with a new approach *via* aortotomy recently described.[79]

Although those results are encouraging, like undersized annuloplasty left ventricular remodeling is not addressed with this technique.

Chordal translocation

Chordal translocation was proposed by Masuyama et al.[80, 81] as an alternative to chordal cutting. The rationale for this technique is to cut the tethering strut cord and to replace them with a suture so that the leaflet coaptation is maximized and the ventricular-valvular continuity preserved. Some authors indeed consider that chordal cutting alone may alter ventricular function,[77, 80] however the animal model used is debatable and these conclusions do not permit the affirmation of the superiority of one procedure over the other one.

b. Surgical Ventricular Reconstruction

Surgical Ventricular Restoration (SVR or Dor procedure) aim to restore normal left ventricular geometry *via* reconstruction. Revascularization is usually performed concomitantly with or without mitral valve repair if needed. Most of the patients chosen for this aggressive surgical procedure suffer from heart failure either from advanced degenerative or ischemic etiology and may benefit from transplantation.[82] The left ventricular volume is reduced by plication of redundant dilated left ventricular wall.[83]

Several studies focused on the role of SVR for FMR. Di Donato et al.[84] found a surprisingly high survival rate of 88 percent at three years for patients undergoing SVR and CABG, however their study population included only patients with mild chronic FMR secondary to anterior myocardial infarction. They did comment on the fact that the valvular complex was not directly involved in the ischemic zone. MR was secondary to

more global left ventricular remodeling. They hypothesized that they could reconstruct the geometry of the mitral valve complex. They did not perform a valve repair. Perhaps, their success rate can be explained by their rigorous case selection. Prucz et al.[82] however did include a larger population and compared the impact of SVR and CABG to CABG alone on chronic ischemic MR. SVR did reduce the MR but survival rates were similar. Patients undergoing SVR and CABG were less likely to be readmitted in the hospital for CHF.

c. Repositioning of the papillary muscles

Procedures requiring bypass surgery

Kron et al.[85] first introduced the concept of relocating the posterior papillary muscle during an open approach. The rationale is that tethering of the posterior papillary muscle can be reduced and maintained stable by a permanent suture to the fixed

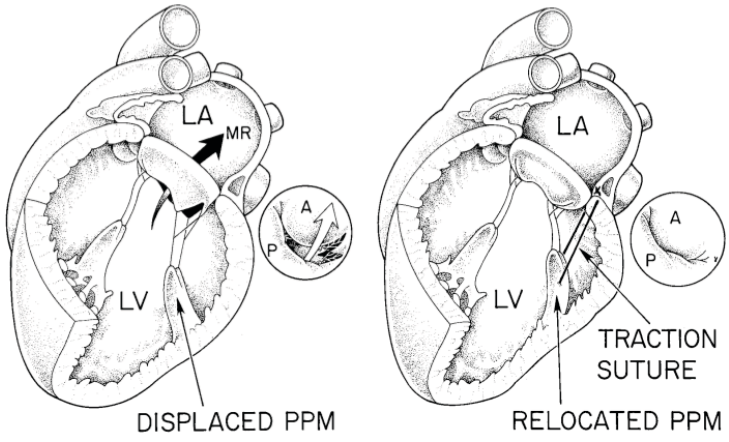

Figure 4.8: Kron suture. Left: apical displacement of the posterior papillary muscle (PPM) causes mitral regurgitation (MR), right: relocation of the posterior papillary muscle restores adequate coaptation of the aortic (A) and mural (P) mitral leaflets. LV: left ventricle, LA: left atrium. Kron et al. 2002

annuloplasty ring (Figure 4.8). The short term result reported in a brief communication[86] seems encouraging. Rama et al.[87] introduced a variant of the Kron suture. They sutured

the two papillary muscle together, placing the tips in the median plane. They tested their method in eight patients with advanced ischemic cardiomyopathy and MR who underwent concomitant undersized annuloplasty. Six patients were alive with absent to mild MR at approximatively one year follow-up. The low number of patients did not allow a statistical analysis.

Surgical procedures on beating heart

Moainie et al.[88] used an epicardial patch prophylactically sutured over an infarcted area. The patch reduced the MR compared to the control group but could not prevent it. Hung et al.[89] reused the idea of an epicardial patch but did upgrade it with the addition of an inflatable balloon (Figure 4.9). They demonstrated that MR could be

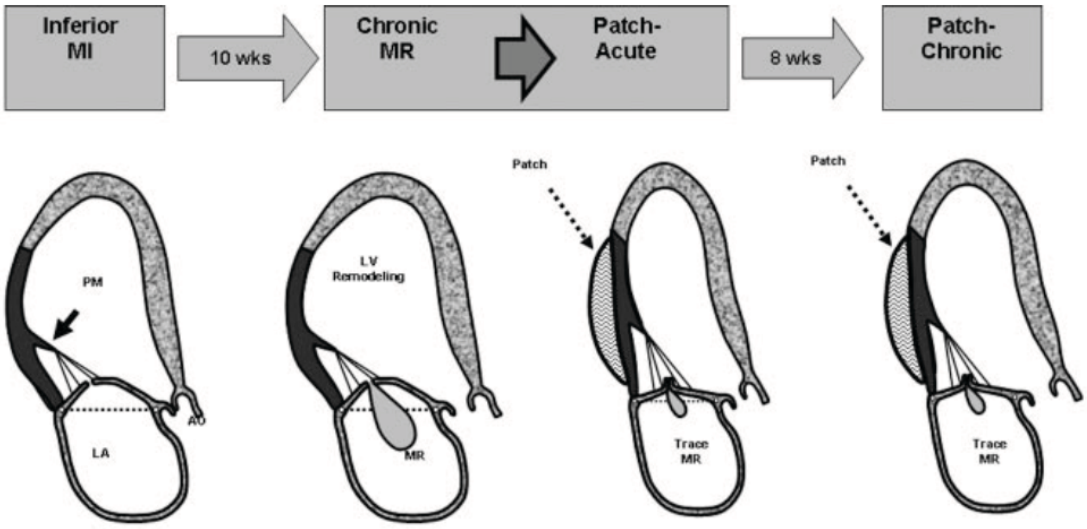

Figure 4.9: Papillary muscle repositioning with an epicardial patch balloon. Hung et al. 2007

corrected by repositioning the papillary muscle *via* external pressure. Interestingly, they reported that the patch-balloon did not change the indexes of left ventricular contractility, stiffness and relaxation time constant either in the acute or chronic phase. Left

ventricular remodeling with increased left ventricular volumes did happen in half of the animals.

The same research team tested an alternative procedure for papillary muscle repositioning by injection of Polyvinyl Alcohol (PVA) gel into the myocardium.[90] The bulging created at the level of the posterior papillary muscle decreased the tethering and reduced MR to trace amounts in an acute ischemic model.

In a similar aim to replace the papillary muscles by correcting the infarct area, Liel-Cohen et al.[91] reduced MR in a chronic ischemic model by repositioning of the papillary muscles *via* plication of the infarcted region. The sutures were strictly placed over the infarct and the only independent predictor for reduction of MR was the tethering length of the papillary muscle tips.[91] They concluded that very localized geometric changes affecting the mitral valve attachments could be of major benefit for correction of MR.

All of these techniques showed promising results, but so far have only been evaluated in animal models.

The only surgical procedure aimed at repositioning the papillary muscles off-pump sparingly tested in human clinical trials uses the Coapsys device (Myocor, Mapple Groove, Minnesota). Fukamashi et al.[92] originally introduced the Coapsys device designed to reshape the left ventricle and in some degree the annulus in patients with ischemic MR (Figure 4.10). The device is constituted by an anterior pad and a posterior pad linked by an expanded polytetrafluoroethylene coated subvalvular cord. The device is fitted to reduce MR during surgery under echocardiographic visualization.[71, 92] The Coapsys is currently being evaluated in a multi-center randomized prospective study: the Randomized Evaluation of a Surgical Treatment for Off-pump Repair of the Mitral Valve (RESTORE-MV) which compares the efficacy of the device to undersized annuloplasty

in patients undergoing CABG who have FMR.[93] The initial results showed that the device reduced the septo-lateral dimension of the annulus and MR to a similar extent as in the annuloplasty group. However, they did not provide statistical analysis between groups. The anteroposterior dimension of the left ventricle was reduced as well, as opposed to the annuloplasty technique which did not. The index of sphericity was then decreased. They concluded that the Coapsys device could correct MR to the same extend as annuloplasty and reshape the left ventricle in addition.[93]

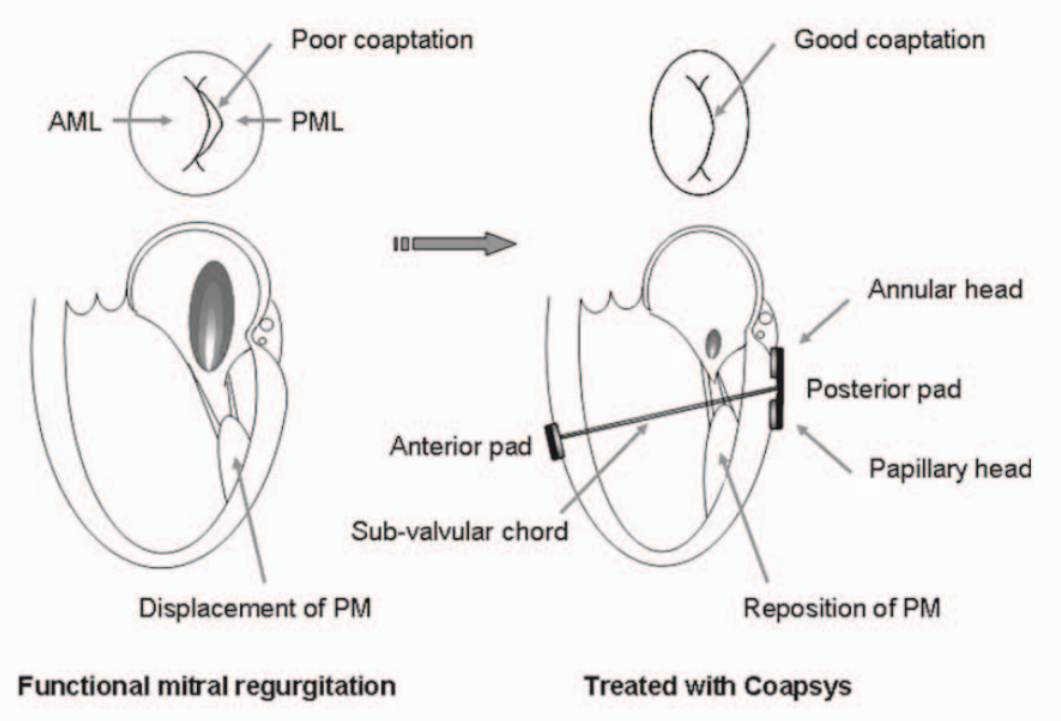

Figure 4.10: Correction of IMR by the Coapsys device. The papillary muscle are drawn together by the annular head of the posterior pad while the papillary muscles are repositioned by the papillary head of the posterior pad. AML: aortic mitral leaflet, PML: mural mitral leaflet, PM: papillary muscle. Fukamachi 2008

One-year follow-up is available for 11 patients from a prospective non randomized single-center feasibility study.[94] They did not report any failure of the implant. The MR remained lower than the baseline level. A percutaneous delivery

system for the Coapsys has been recently described and will be enrolled soon in a feasibility study.[71, 95]

The ability to correct the subvalvular geometry during an off-pump procedure is the main advantage of the device. However, the myocardium is not spared during the device placement: because of its design, the left ventricle has to be perforated which may increase the operative risk in an off-pump procedure. Furthermore, some authors think that the permanent annular cinching may lead to further remodeling and altered transmyocardial strains.[96] Finally, the subvalvular cord may create hemodynamic turbulence increasing the thromboembolic risk for those patients.

3. Benefits of a subvalvular procedure associated with a mitral valve annuloplasty

In a recent retrospective study of 59 patients with ischemic functional MR undergoing surgical correction, Ueno et al.[97] compared the postoperative and mid term echocardiographic findings of three study groups: the patients either had undersized annuloplasty alone, undersized annuloplasty and SVR, or undersized annuloplasty, SVR and a subvalvular procedure (chordal cutting, translocation or papillary muscle approximation). All the patients received a CABG concomitantly with the other procedures. They observed that the additional subvalvular procedures significantly corrected leaflet tethering and maintained a lower mitral regurgitation grade compared to the other groups. Based on their echocardiographic measurements the authors expect a reduced recurrence of MR.

4. Conclusion

Mitral apparatus tethering is the major component leading to functional mitral regurgitation. The current treatment technique of choice is the undersized annuloplasty,

which requires extracorporeal circulation during anesthesia. Furthermore, no technique addresses directly the left ventricular remodeling. Hence, an epicardial device altering the forces applied on the leaflets (figure 3.2) by repositioning the papillary muscles should be beneficial.

Bibliography

1. Lloyd-Jones D, Adams R, Carnethon M, De Simone G, Ferguson TB, Flegal K, Ford E, Furie K, Go A, Greenlund K, Haase N, Hailpern S, Ho M, Howard V, Kissela B, Kittner S, Lackland D, Lisabeth L, Marelli A, McDermott M, Meigs J, Mozaffarian D, Nichol G, O'Donnell C, Roger V, Rosamond W, Sacco R, Sorlie P, Stafford R, Steinberger J, Thom T, Wasserthiel-Smoller S, Wong N, Wylie-Rosett J, Hong Y. Heart disease and stroke statistics--2009 update: a report from the American Heart Association Statistics Committee and Stroke Statistics Subcommittee. *Circulation.* 2009;119(3):480-486.

2. Lamas GA, Mitchell GF, Flaker GC, Smith SC, Jr., Gersh BJ, Basta L, Moye L, Braunwald E, Pfeffer MA. Clinical significance of mitral regurgitation after acute myocardial infarction. Survival and Ventricular Enlargement Investigators. *Circulation.* 1997;96(3): 827-833.

3. Grigioni F, Enriquez-Sarano M, Zehr KJ, Bailey KR, Tajik AJ. Ischemic mitral regurgitation: long-term outcome and prognostic implications with quantitative Doppler assessment. *Circulation.* 2001;103(13):1759-1764.

4. Feinberg MS, Schwammenthal E, Shlizerman L, Porter A, Hod H, Friemark D, Matezky S, Boyko V, Mandelzweig L, Vered Z, Behar S, Sagie A. Prognostic significance of mild mitral regurgitation by color Doppler echocardiography in acute myocardial infarction. *Am J Cardiol.* 2000;86(9):903-907.

5. Kumanohoso T, Otsuji Y, Yoshifuku S, Matsukida K, Koriyama C, Kisanuki A, Minagoe S, Levine RA, Tei C. Mechanism of higher incidence of ischemic mitral regurgitation in patients with inferior myocardial infarction: quantitative analysis of left ventricular and mitral valve geometry in 103 patients with prior myocardial infarction. *J Thorac Cardiovasc Surg.* 2003;125(1):135-143.

6. Amigoni M, Meris A, Thune JJ, Mangalat D, Skali H, Bourgoun M, Warnica JW, Barvik S, Arnold JM, Velazquez EJ, Van de Werf F, Ghali J, McMurray JJ, Kober L, Pfeffer MA, Solomon SD. Mitral regurgitation in myocardial infarction complicated by heart failure, left ventricular dysfunction, or both: prognostic significance and relation to ventricular size and function. *European heart journal.* 2007;28(3):326-333.

7. Gorman JH, 3rd, Gupta KB, Streicher JT, Gorman RC, Jackson BM, Ratcliffe MB, Bogen DK, Edmunds LH, Jr. Dynamic three-dimensional imaging of the mitral valve and left ventricle by rapid sonomicrometry array localization. *J Thorac Cardiovasc Surg.* 1996;112 (3):712-726.

8. Llaneras MR, Nance ML, Streicher JT, Lima JA, Savino JS, Bogen DK, Deac RF, Ratcliffe MB, Edmunds LH, Jr. Large animal model of ischemic mitral regurgitation. *Ann Thorac Surg.* 1994;57(2):432-439.

9. Hasnat AK, van der Velde ET, Hon JK, Yacoub MH. Reproducible model of post-infarction left ventricular dysfunction: haemodynamic characterization by conductance catheter. *Eur J Cardiothorac Surg.* 2003;24(1):98-104.

10. Angelini A, Ho SY, Anderson RH, Davies MJ, Becker AE. A histological study of the atrioventricular junction in hearts with normal and prolapsed leaflets of the mitral valve. *Br Heart J.* 1988;59(6):712-716.

11. Levine RA, Handschumacher MD, Sanfilippo AJ, Hagege AA, Harrigan P, Marshall JE, Weyman AE. Three-dimensional echocardiographic reconstruction of the mitral valve, with implications for the diagnosis of mitral valve prolapse. *Circulation.* 1989;80(3): 589-598.

12. Kwan J, Shiota T, Agler DA, Popovic ZB, Qin JX, Gillinov MA, Stewart WJ, Cosgrove DM, McCarthy PM, Thomas JD. Geometric differences of the mitral apparatus between ischemic and dilated cardiomyopathy with significant mitral regurgitation: real-time three-dimensional echocardiography study. *Circulation.* 2003;107(8):1135-1140.

13. Salgo IS, Gorman JH, 3rd, Gorman RC, Jackson BM, Bowen FW, Plappert T, St John Sutton MG, Edmunds LH, Jr. Effect of annular shape on leaflet curvature in reducing mitral leaflet stress. *Circulation.* 2002;106(6):711-717.

14. Muresian H. The clinical anatomy of the mitral valve. *Clin Anat.* 2009;22(1):85-98.

15. Ho SY. Anatomy of the mitral valve. *Heart.* 2002;88 Suppl 4:iv5-10.

16. Roberts WC. Morphologic features of the normal and abnormal mitral valve. *Am J Cardiol.* 1983;51(6):1005-1028.

17. Chen L, May-Newman K. Effect of strut chordae transection on mitral valve leaflet biomechanics. *Ann Biomed Eng.* 2006;34(6):917-926.

18. Nielsen SL, Nygaard H, Mandrup L, Fontaine AA, Hasenkam JM, He S, Yoganathan AP. Mechanism of incomplete mitral leaflet coaptation--interaction of chordal restraint and changes in mitral leaflet coaptation geometry. Insight from in vitro validation of the premise of force equilibrium. *J Biomech Eng.* 2002;124(5):596-608.

19. Estes EH, Jr., Dalton FM, Entman ML, Dixon HB, 2nd, Hackel DB. The anatomy and blood supply of the papillary muscles of the left ventricle. *Am Heart J.* 1966;71(3): 356-362.

20. Voci P, Bilotta F, Caretta Q, Mercanti C, Marino B. Papillary muscle perfusion pattern. A hypothesis for ischemic papillary muscle dysfunction. *Circulation.* 1995;91(6):1714-1718.

21. Dagum P, Timek TA, Green GR, Lai D, Daughters GT, Liang DH, Hayase M, Ingels NB, Jr., Miller DC. Coordinate-free analysis of mitral valve dynamics in normal and ischemic hearts. *Circulation.* 2000;102(19 Suppl 3):III62-69.

22. Lai DT, Tibayan FA, Myrmel T, Timek TA, Dagum P, Daughters GT, Liang D, Ingels NB, Jr., Miller DC. Mechanistic insights into posterior mitral leaflet inter-scallop malcoaptation during acute ischemic mitral regurgitation. *Circulation.* 2002;106(12 Suppl 1):I40-I45.

23. Nazari S, Carli F, Salvi S, Banfi C, Aluffi A, Mourad Z, Buniva P, Rescigno G. Patterns of systolic stress distribution on mitral valve anterior leaflet chordal apparatus. A structural mechanical theoretical analysis. *J Cardiovasc Surg (Torino).* 2000;41(2):193-202.

24. Joudinaud TM, Kegel CL, Flecher EM, Weber PA, Lansac E, Hvass U, Duran CM. The papillary muscles as shock absorbers of the mitral valve complex. An experimental study. *Eur J Cardiothorac Surg.* 2007;32(1):96-101.

25. Otsuji Y, Handschumacher MD, Liel-Cohen N, Tanabe H, Jiang L, Schwammenthal E, Guerrero JL, Nicholls LA, Vlahakes GJ, Levine RA. Mechanism of ischemic mitral regurgitation with segmental left ventricular dysfunction: three-dimensional echocardiographic studies in models of acute and chronic progressive regurgitation. *Journal of the American College of Cardiology.* 2001;37(2):641-648.

26. Kaul S, Spotnitz WD, Glasheen WP, Touchstone DA. Mechanism of ischemic mitral regurgitation. An experimental evaluation. *Circulation.* 1991;84(5):2167-2180.

27. Messas E, Guerrero JL, Handschumacher MD, Chow CM, Sullivan S, Schwammenthal E, Levine RA. Paradoxic decrease in ischemic mitral regurgitation with papillary muscle dysfunction: insights from three-dimensional and contrast echocardiography with strain rate measurement. *Circulation.* 2001;104(16):1952-1957.

28. Mittal AK, Langston M, Jr., Cohn KE, Selzer A, Kerth WJ. Combined papillary muscle and left ventricular wall dysfunction as a cause of mitral regurgitation. An experimental study. *Circulation.* 1971;44(2):174-180.

29. Timek TA, Lai DT, Tibayan F, Liang D, Daughters GT, Dagum P, Zasio MK, Lo S, Hastie T, Ingels NB, Jr., Miller DC. Ischemia in three left ventricular regions: Insights into the pathogenesis of acute ischemic mitral regurgitation. *The Journal of thoracic and cardiovascular surgery.* 2003;125(3):559-569.

30. Gorman JH, 3rd, Jackson BM, Enomoto Y, Gorman RC. The effect of regional ischemia on mitral valve annular saddle shape. *Ann Thorac Surg.* 2004;77(2):544-548.

31. Glasson JR, Komeda M, Daughters GT, Bolger AF, Karlsson MO, Foppiano LE, Hayase M, Oesterle SN, Ingels NB, Jr., Miller DC. Early systolic mitral leaflet "loitering" during acute ischemic mitral regurgitation. *J Thorac Cardiovasc Surg.* 1998;116(2):193-205.

32. Timek TA, Lai DT, Liang D, Tibayan F, Langer F, Rodriguez F, Daughters GT, Ingels NB, Jr., Miller DC. Effects of paracommissural septal-lateral annular cinching on acute ischemic mitral regurgitation. *Circulation.* 2004;110(11 Suppl 1):II79-84.

33. Tibayan FA, Rodriguez F, Zasio MK, Bailey L, Liang D, Daughters GT, Langer F, Ingels NB, Jr., Miller DC. Geometric distortions of the mitral valvular-ventricular complex in chronic ischemic mitral regurgitation. *Circulation.* 2003;108 Suppl 1:II116-121.

34. Park SM, Park SW, Casaclang-Verzosa G, Ommen SR, Pellikka PA, Miller FA, Jr., Sarano ME, Kubo SH, Oh JK. Diastolic dysfunction and left atrial enlargement as contributing factors to functional mitral regurgitation in dilated cardiomyopathy: data from the Acorn trial. *Am Heart J.* 2009;157(4):762 e763-710.

35. Otsuji Y, Kumanohoso T, Yoshifuku S, Matsukida K, Koriyama C, Kisanuki A, Minagoe S, Levine RA, Tei C. Isolated annular dilation does not usually cause important functional mitral regurgitation: comparison between patients with lone atrial fibrillation and those with idiopathic or ischemic cardiomyopathy. *J Am Coll Cardiol.* 2002;39(10):1651-1656.

36. Green GR, Dagum P, Glasson JR, Daughters GT, Bolger AF, Foppiano LE, Berry GJ, Ingels NB, Jr., Miller DC. Mitral annular dilatation and papillary muscle dislocation without mitral regurgitation in sheep. *Circulation.* 1999;100(19 Suppl):II95-102.

37. Tibayan FA, Wilson A, Lai DT, Timek TA, Dagum P, Rodriguez F, Zasio MK, Liang D, Daughters GT, Ingels NB, Jr., Miller DC. Tenting volume: three-dimensional assessment of geometric perturbations in functional mitral regurgitation and implications for surgical repair. *The Journal of heart valve disease.* 2007;16(1):1-7.

38. Ryan LP, Jackson BM, Parish LM, Sakamoto H, Plappert TJ, St John-Sutton M, Gorman JH, 3rd, Gorman RC. Mitral valve tenting index for assessment of subvalvular remodeling. *Ann Thorac Surg.* 2007;84(4):1243-1249.

39. Otsuji Y, Handschumacher MD, Schwammenthal E, Jiang L, Song JK, Guerrero JL, Vlahakes GJ, Levine RA. Insights from three-dimensional echocardiography into the mechanism of functional mitral regurgitation: direct in vivo demonstration of altered leaflet tethering geometry. *Circulation.* 1997;96(6):1999-2008.

40. He S, Fontaine AA, Schwammenthal E, Yoganathan AP, Levine RA. Integrated mechanism for functional mitral regurgitation: leaflet restriction versus coapting force: in vitro studies. *Circulation.* 1997;96(6):1826-1834.

41. Izumi S, Miyatake K, Beppu S, Park YD, Nagata S, Kinoshita N, Sakakibara H, Nimura Y. Mechanism of mitral regurgitation in patients with myocardial infarction: a study using real-time two-dimensional Doppler flow imaging and echocardiography. *Circulation.* 1987;76(4):777-785.

42. Schwammenthal E, Popescu AC, Popescu BA, Freimark D, Hod H, Eldar M, Feinberg MS. Mechanism of mitral regurgitation in inferior wall acute myocardial infarction. *Am J Cardiol.* 2002;90(3):306-309.

43. May-Newman K, Yin FC. Biaxial mechanical behavior of excised porcine mitral valve leaflets. *Am J Physiol.* 1995;269(4 Pt 2):H1319-1327.

44. Grande-Allen KJ, Borowski AG, Troughton RW, Houghtaling PL, Dipaola NR, Moravec CS, Vesely I, Griffin BP. Apparently normal mitral valves in patients with heart failure demonstrate biochemical and structural derangements: an extracellular matrix and echocardiographic study. *J Am Coll Cardiol.* 2005;45(1):54-61.

45. Chaput M, Handschumacher MD, Tournoux F, Hua L, Guerrero JL, Vlahakes GJ, Levine RA. Mitral leaflet adaptation to ventricular remodeling: occurrence and adequacy in patients with functional mitral regurgitation. *Circulation.* 2008;118(8):845-852.

46. Dal-Bianco JP, Aikawa E, Bischoff J, Guerrero JL, Handschumacher MD, Sullivan S, Johnson B, Titus JS, Iwamoto Y, Wylie-Sears J, Levine RA, Carpentier A. Active adaptation of the tethered mitral valve: insights into a compensatory mechanism for functional mitral regurgitation. *Circulation.* 2009;120(4):334-342.

47. Fornes P, Heudes D, Fuzellier JF, Tixier D, Bruneval P, Carpentier A. Correlation between clinical and histologic patterns of degenerative mitral valve insufficiency: a histomorphometric study of 130 excised segments. *Cardiovasc Pathol.* 1999;8(2):81-92.

48. Quick DW, Kunzelman KS, Kneebone JM, Cochran RP. Collagen synthesis is upregulated in mitral valves subjected to altered stress. *ASAIO J.* 1997;43(3):181-186.

49. Trichon BH, Felker GM, Shaw LK, Cabell CH, O'Connor CM. Relation of frequency and severity of mitral regurgitation to survival among patients with left ventricular systolic dysfunction and heart failure. *Am J Cardiol.* 2003;91(5):538-543.

50. Raja SG, Berg GA. Moderate ischemic mitral regurgitation: to treat or not to treat? *Journal of cardiac surgery.* 2007;22(4):362-369.

51. Kay GL, Kay JH, Zubiate P, Yokoyama T, Mendez M. Mitral valve repair for mitral regurgitation secondary to coronary artery disease. *Circulation.* 1986;74(3 Pt 2):I88-98.

52. Gillinov AM, Wierup PN, Blackstone EH, Bishay ES, Cosgrove DM, White J, Lytle BW, McCarthy PM. Is repair preferable to replacement for ischemic mitral regurgitation? *J Thorac Cardiovasc Surg.* 2001;122(6):1125-1141.

53. Bolling SF, Pagani FD, Deeb GM, Bach DS. Intermediate-term outcome of mitral reconstruction in cardiomyopathy. *The Journal of thoracic and cardiovascular surgery.* 1998;115(2):381-386; discussion 387-388.

54. McGee EC, Gillinov AM, Blackstone EH, Rajeswaran J, Cohen G, Najam F, Shiota T, Sabik JF, Lytle BW, McCarthy PM, Cosgrove DM. Recurrent mitral regurgitation after annuloplasty for functional ischemic mitral regurgitation. *J Thorac Cardiovasc Surg.* 2004;128(6):916-924.

55. Bolling SF, Deeb GM, Bach DS. Mitral valve reconstruction in elderly, ischemic patients. *Chest.* 1996;109(1):35-40.

56. Gorman JH, 3rd, Ryan LP, Gorman RC. Pathophysiology of ischemic mitral insufficiency: does repair make a difference? *Heart failure reviews.* 2006;11(3):219-229.

57. Aklog L, Filsoufi F, Flores KQ, Chen RH, Cohn LH, Nathan NS, Byrne JG, Adams DH. Does coronary artery bypass grafting alone correct moderate ischemic mitral regurgitation? *Circulation.* 2001;104(12 Suppl 1):I68-75.

58. Borger MA, Alam A, Murphy PM, Doenst T, David TE. Chronic ischemic mitral regurgitation: repair, replace or rethink? *Ann Thorac Surg.* 2006;81(3):1153-1161.

59. Harris KM, Sundt TM, 3rd, Aeppli D, Sharma R, Barzilai B. Can late survival of patients with moderate ischemic mitral regurgitation be impacted by intervention on the valve? *Ann Thorac Surg.* 2002;74(5):1468-1475.

60. Diodato MD, Moon MR, Pasque MK, Barner HB, Moazami N, Lawton JS, Bailey MS, Guthrie TJ, Meyers BF, Damiano RJ, Jr. Repair of ischemic mitral regurgitation does not increase mortality or improve long-term survival in patients undergoing coronary artery revascularization: a propensity analysis. *Ann Thorac Surg.* 2004;78(3):794-799; discussion 794-799.

61. Guy TSt, Moainie SL, Gorman JH, 3rd, Jackson BM, Plappert T, Enomoto Y, St John-Sutton MG, Edmunds LH, Jr., Gorman RC. Prevention of ischemic mitral regurgitation does not influence the outcome of remodeling after posterolateral myocardial infarction. *Journal of the American College of Cardiology.* 2004;43(3):377-383.

62. Enomoto Y, Gorman JH, 3rd, Moainie SL, Guy TS, Jackson BM, Parish LM, Plappert T, Zeeshan A, St John-Sutton MG, Gorman RC. Surgical treatment of ischemic mitral regurgitation might not influence ventricular remodeling. *The Journal of thoracic and cardiovascular surgery.* 2005;129(3):504-511.

63. Hung J, Papakostas L, Tahta SA, Hardy BG, Bollen BA, Duran CM, Levine RA. Mechanism of recurrent ischemic mitral regurgitation after annuloplasty: continued LV remodeling as a moving target. *Circulation.* 2004;110(11 Suppl 1):II85-90.

64. Onorati F, Rubino AS, Marturano D, Pasceri E, Santarpino G, Zinzi S, Mascaro G, Renzulli A. Midterm clinical and echocardiographic results and predictors of mitral regurgitation recurrence following restrictive annuloplasty for ischemic cardiomyopathy. *J Thorac Cardiovasc Surg.* 2009;138(3):654-662.

65. Lee AP, Acker M, Kubo SH, Bolling SF, Park SW, Bruce CJ, Oh JK. Mechanisms of recurrent functional mitral regurgitation after mitral valve repair in nonischemic dilated cardiomyopathy: importance of distal anterior leaflet tethering. *Circulation.* 2009;119(19): 2606-2614.

66. Alfieri O, Maisano F, De Bonis M, Stefano PL, Torracca L, Oppizzi M, La Canna G. The double-orifice technique in mitral valve repair: a simple solution for complex problems. *J Thorac Cardiovasc Surg.* 2001;122(4):674-681.

67. Maisano F, Caldarola A, Blasio A, De Bonis M, La Canna G, Alfieri O. Midterm results of edge-to-edge mitral valve repair without annuloplasty. *J Thorac Cardiovasc Surg.* 2003;126(6):1987-1997.

68. Bhudia SK, McCarthy PM, Smedira NG, Lam BK, Rajeswaran J, Blackstone EH. Edge-to-edge (Alfieri) mitral repair: results in diverse clinical settings. *Ann Thorac Surg.* 2004;77(5):1598-1606.

69. Fann JI, St Goar FG, Komtebedde J, Oz MC, Block PC, Foster E, Butany J, Feldman T, Burdon TA. Beating heart catheter-based edge-to-edge mitral valve procedure in a porcine model: efficacy and healing response. *Circulation.* 2004;110(8):988-993.

70. Fundaro P, Pocar M, Moneta A, Donatelli F, Grossi A. Posterior mitral valve restoration for ischemic regurgitation. *Ann Thorac Surg.* 2004;77(2):729-730.

71. Fukamachi K. Percutaneous and off-pump treatments for functional mitral regurgitation. *J Artif Organs.* 2008;11(1):12-18.

72. Maselli D, Guarracino F, Chiaramonti F, Mangia F, Borelli G, Minzioni G. Percutaneous mitral annuloplasty: an anatomic study of human coronary sinus and its relation with mitral valve annulus and coronary arteries. *Circulation.* 2006;114(5):377-380.

73. Messas E, Guerrero JL, Handschumacher MD, Conrad C, Chow CM, Sullivan S, Yoganathan AP, Levine RA. Chordal cutting: a new therapeutic approach for ischemic mitral regurgitation. *Circulation.* 2001;104(16):1958-1963.

74. Messas E, Pouzet B, Touchot B, Guerrero JL, Vlahakes GJ, Desnos M, Menasche P, Hagege A, Levine RA. Efficacy of chordal cutting to relieve chronic persistent ischemic mitral regurgitation. *Circulation.* 2003;108 Suppl 1:II111-115.

75. Messas E, Yosefy C, Chaput M, Guerrero JL, Sullivan S, Menasche P, Carpentier A, Desnos M, Hagege AA, Vlahakes GJ, Levine RA. Chordal cutting does not adversely affect left ventricle contractile function. *Circulation.* 2006;114(1 Suppl):I524-528.

76. Moon MR, DeAnda A, Jr., Daughters GT, 2nd, Ingels NB, Miller DC. Effects of chordal disruption on regional left ventricular torsional deformation. *Circulation.* 1996;94(9 Suppl):II143-151.

77. Rodriguez F, Langer F, Harrington KB, Tibayan FA, Zasio MK, Liang D, Daughters GT, Ingels NB, Miller DC. Cutting second-order chords does not prevent acute ischemic mitral regurgitation. *Circulation.* 2004;110(11 Suppl 1):II91-97.

78. Borger MA, Murphy PM, Alam A, Fazel S, Maganti M, Armstrong S, Rao V, David TE. Initial results of the chordal-cutting operation for ischemic mitral regurgitation. *The Journal of thoracic and cardiovascular surgery.* 2007;133(6):1483-1492.

79. Fayad G, Modine T, Azzaoui R, Larrue B, Cracco A, Pansard E, Decoene C, Warembourg H. Chordal cutting technique through aortotomy to treat chronic ischemic mitral regurgitation: surgical technique. *Int J Surg.* 2008;6(1):36-39.

80. Masuyama S, Marui A, Shimamoto T, Nonaka M, Tsukiji M, Watanabe N, Ikeda T, Yoshida K, Komeda M. Chordal translocation for ischemic mitral regurgitation may ameliorate tethering of the posterior and anterior mitral leaflets. *J Thorac Cardiovasc Surg.* 2008;136 (4):868-875.

81. Masuyama S, Marui A, Shimamoto T, Komeda M. Chordal translocation: secondary chordal cutting in conjunction with artificial chordae for preserving valvular-ventricular interaction in the treatment of functional mitral regurgitation. *J Heart Valve Dis.* 2009;18 (2):142-146.

82. Prucz RB, Weiss ES, Patel ND, Nwakanma LU, Shah AS, Conte JV. The impact of surgical ventricular restoration on mitral valve regurgitation. *Ann Thorac Surg.* 2008;86 (3):726-734; discussion 726-734.

83. Patel ND, Barreiro CJ, Williams JA, Bonde PN, Waldron M, Natori S, Bluemke DA, Conte JV. Surgical ventricular remodeling for patients with clinically advanced congestive heart failure and severe left ventricular dysfunction. *J Heart Lung Transplant.* 2005;24(12): 2202-2210.

84. Di Donato M, Castelvecchio S, Brankovic J, Santambrogio C, Montericcio V, Menicanti L. Effectiveness of surgical ventricular restoration in patients with dilated ischemic cardiomyopathy and unrepaired mild mitral regurgitation. *J Thorac Cardiovasc Surg.* 2007;134(6):1548-1553.

85. Kron IL, Green GR, Cope JT. Surgical relocation of the posterior papillary muscle in chronic ischemic mitral regurgitation. *The Annals of thoracic surgery.* 2002;74(2):600-601.

86. Langer F, Schafers HJ. RING plus STRING: papillary muscle repositioning as an adjunctive repair technique for ischemic mitral regurgitation. *J Thorac Cardiovasc Surg.* 2007;133(1):247-249.

87. Rama A, Praschker L, Barreda E, Gandjbakhch I. Papillary muscle approximation for functional ischemic mitral regurgitation. *The Annals of thoracic surgery.* 2007;84(6): 2130-2131.

88. Moainie SL, Guy TS, Gorman JH, 3rd, Plappert T, Jackson BM, St John-Sutton MG, Edmunds LH, Jr., Gorman RC. Infarct restraint attenuates remodeling and reduces chronic ischemic mitral regurgitation after postero-lateral infarction. *The Annals of thoracic surgery.* 2002;74(2):444-449; discussion 449.

89. Hung J, Chaput M, Guerrero JL, Handschumacher MD, Papakostas L, Sullivan S, Solis J, Levine RA. Persistent reduction of ischemic mitral regurgitation by papillary muscle repositioning: structural stabilization of the papillary muscle-ventricular wall complex. *Circulation.* 2007;116(11 Suppl):I259-263.

90. Hung J, Solis J, Guerrero JL, Braithwaite GJ, Muratoglu OK, Chaput M, Fernandez-Friera L, Handschumacher MD, Wedeen VJ, Houser S, Vlahakes GJ, Levine RA. A novel approach for reducing ischemic mitral regurgitation by injection of a polymer to reverse remodel and reposition displaced papillary muscles. *Circulation.* 2008;118(14 Suppl):S263-269.

91. Liel-Cohen N, Guerrero JL, Otsuji Y, Handschumacher MD, Rudski LG, Hunziker PR, Tanabe H, Scherrer-Crosbie M, Sullivan S, Levine RA. Design of a new surgical approach for ventricular remodeling to relieve ischemic mitral regurgitation: insights from 3-dimensional echocardiography. *Circulation.* 2000;101(23):2756-2763.

92. Fukamachi K, Inoue M, Popovic ZB, Doi K, Schenk S, Nemeh H, Ootaki Y, Kopcak MW, Jr., Dessoffy R, Thomas JD, Bianco RW, Berry JM, McCarthy PM. Off-pump mitral valve repair using the Coapsys device: a pilot study in a pacing-induced mitral regurgitation model. *Ann Thorac Surg.* 2004;77(2):688-692; discussion 692-683.

93. Grossi EA, Woo YJ, Schwartz CF, Gangahar DM, Subramanian VA, Patel N, Wudel J, DiGiorgi PL, Singh A, Davis RD. Comparison of Coapsys annuloplasty and internal reduction mitral annuloplasty in the randomized treatment of functional ischemic mitral regurgitation: impact on the left ventricle. *J Thorac Cardiovasc Surg.* 2006;131(5): 1095-1098.

94. Mishra YK, Mittal S, Jaguri P, Trehan N. Coapsys mitral annuloplasty for chronic functional ischemic mitral regurgitation: 1-year results. *Ann Thorac Surg.* 2006;81(1): 42-46.

95. Pedersen WR, Block P, Leon M, Kramer P, Kapadia S, Babaliaros V, Kodali S, Tuzcu EM, Feldman T. iCoapsys mitral valve repair system: Percutaneous implantation in an animal model. *Catheter Cardiovasc Interv.* 2008;72(1):125-131.

96. Nguyen TC, Cheng A, Tibayan FA, Liang D, Daughters GT, Ingels NB, Jr., Miller DC. Septal-lateral annnular cinching perturbs basal left ventricular transmural strains. *Eur J Cardiothorac Surg.* 2007;31(3):423-429.

97. Ueno T, Sakata R, Iguro Y, Yamamoto H, Ueno M, Matsumoto K, Hisashi Y, Tei C. Impact of subvalvular procedure for ischemic mitral regurgitation on leaflet configuration, mobility, and recurrence. *Circ J.* 2008;72(11):1737-1743.

Chapter V

Evaluation of an acute model of myocardial ischemia to induce functional mitral valve regurgitation in sheep: Evaluation of diastolic dysfunction

Regional and global systolic dysfunction associated with acute myocardial infarction (AMI) are widely recognized as independent predictors of prognosis,[1-3] however, the role diastolic dysfunction remains unclear. Diastolic wall motion abnormalities may be transient and can regress overtime post treatment of AMI.[4-6] Systolic and diastolic heart failure represent different entity of heart failure.[7, 8] Systolic and diastolic dysfunction after AMI may arise from a similar cellular level.[5, 6] Long term outcome and remodeling after myocardial infarction has been widely evaluated and studied. Diastolic dysfunction after myocardial ischemia is a well recognized problem that might even develop in the absence of systolic dysfunction. However, diastolic dysfunction in the acute phase of myocardial ischemia has not been evaluated.

1. Hypothesis

The purpose of our study was to evaluate acute myocardial ischemia to induce functional mitral valve regurgitation and evaluate global and regional left ventricular function and compliance in an acute ovine model of regional supply ischemia.

2. *Material and methods*

The experimental protocol used for this investigation received the approval of the Animal Care and Use Committee (#: 07-003A-01) at Colorado State University (Fort Collins, CO, USA).

i. Surgical preparation

Six adult female Dorsett sheep were premedicated with diazepam (7.5 mg IV) and induced with ketamine (250 mg IV). After endotracheal intubation, they were ventilated and maintained under anesthesia with continuous administration of Isoflurane (1.5 to 3%). Fentanyl (20 µg/kg/h IV) and Lidocaine (100 mg/kg/min IV) were continually infused. Left chest-wall resection and subtotal pericardectomy were performed. A bolus of magnesium chloride (1g IV) was injected half an hour after the beginning of the surgery before induction of ischemia. An intercostal thoracotomy was performed. The pericardium was opened.

A high fidelity microtip pressure catheter with two pressure sensors (Pressure Mikro-Tip®, Millar instruments Inc., Houston, USA) was inserted in the left ventricle and proximal aorta through an incision at the apex of the heart. An 18 Gauge catheter was inserted in the left atrium. Four 2 mm ultrasonic crystals (SonometricsCorp., London, Canada) were implanted in the epicardium to measure the major and minor axis of the left ventricle. The minor axis is defined between the left anterior descending coronary artery and the left posterior descending coronary artery, distal to the coronary sinus (Figure 5.11). An aortic flow probe was placed after dissection of the proximal ascending aorta. A 16 Gauge catheter was inserted in the descending aorta. A Rummel tourniquet was placed around the caudal vena cava to induce transient reduction of preload during pressure volume loop recording.

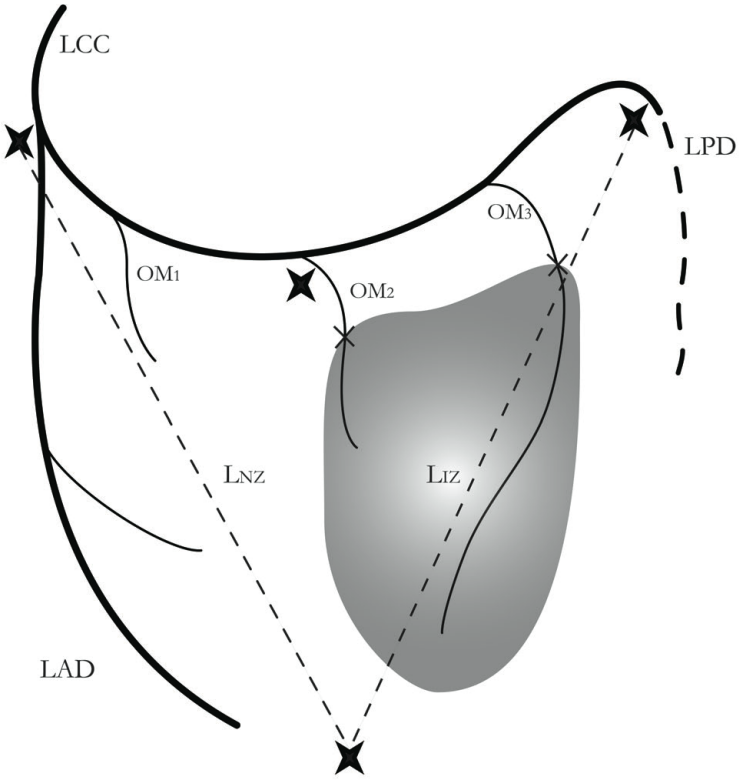

Figure 5.1: Schematic representation of the left ventricular vascularization. LCC: Left Circumflex Coronary artery, LAD: Left Anterior Descending coronary artery, LPD: Left Posterior Descending coronary artery, OM1,2,3: first, second and third Obtuse Marginal branch of the LCC, LNZ and LIZ: axis for the measurement of the non ischemic and ischemic segmental lengths, cross on OM2 and OM3: position of ligatures, grey zone: ischemic area, stars: position of the subepicardial ultrasonic crystals.

The second and third Obtuse Marginal (OM2 and OM3) branch of the left circumflex coronary artery were dissected proximally and two Rummel tourniquets were placed.

At the end of the experiment, the animals were euthanized by injection of 20 mL of pentobarbital IV.

ii. Experimental design and data acquisition.

All the signals from the transducers were recorded and analyzed by a data acquisition software (Sonosoft® Sonometrics Corp., London, Canada). Three sets of recordings were obtained for each sheep, after stabilization of the heart rate. Baseline data was saved following the instrumentation, five to ten minutes after occlusion of OM2 and OM3 the early ischemic data (t + 5-10 min) was recorded and after one hour of occlusion, the late ischemic data (t + 60 min) was saved. For each data recording, the ventilation was stopped and the vena cava gradually occluded in order to calculate the load-dependent indexes by linear regression.

Data was later analyzed by data analysis software (Cardiosoft, SonometricsCorp., London, Canada). The heart rate (HR) was calculated based on the recorded electrocardiogram. End-systole was defined as the maximum ratio of left ventricular pressure (LVP) to left ventricular volume (LVV). End-diastole was defined at the end of the left atrial contraction isolated from the LVP curve. End-Systolic Left Ventricular Pressure (ESLVP), End-Diastolic Left Ventricular Pressure (EDLVP), Aortic Diastolic Pressure (ADP), Aortic Systolic Pressure (ASP) were recorded with the Millar catheter. End-Diastolic Left Ventricular Volume (EDLVV) and End-Systolic Left Ventricular Volume (ESLVV) were calculated based on the ultrasonic crystals calculations using an ellipsoid model. The Stroke Volume (SV) was calculated based on the equation: SV=LVEDV-LVESV. Aortic blood flow (ABF) was recorded and the Aortic Stroke Volume (ASV) calculated based on the equation ASV=ABF/HR. The Mitral Regurgitant volume (MRV) was then defined as: MRV=SV-ASV.

End-Systolic Pressure Volume Relationship (ESPVR) was calculated by linear regression based on the Pressure-Volume curves obtained during transient caval occlusion. End-Diastolic Pressure Volume Relationship (EDPVR) was also calculated

during transient vena cava occlusion. The equation was obtained by exponential regression, fitting $LVP=b0+b1*\exp^{\beta LVV}$ were b0 is the intercept of the LVP value, b1 a curve fitting parameter, LVV the left ventricular volume and β the passive diastolic left ventricular stiffness. External work (EW) of the left ventricle was the area of the Pressure-Volume loop. Pressure-Volume Area (PVA) was defined as the area under ESPVR, above EDPVR and left of the isovolumetric contraction phase of the pressure-volume loop. Emax was defined as the slope of the ESPVR, while V_0 was the intercept with the volume axis. Preload Recruitable Stroke Work (PRSW) was defined as the slope relating EW to LVEDV in the equation: $EW=PRSW*(LVEDV-V_1)$ were V_1 is the intercept with the volume axis. EDPVR, ESPVR and PRSW were calculated by regression based on the Pressure-Volume loops recorded during acute occlusion of the caudal vena cava. Contractile Efficiency (CE) was the ratio between EW and PVA. The first derivative of left ventricle pressure curve against time was used to determine dP/dt max. The left ventricular exponential time constant of isovolumic relaxation τ was calculated by performing a linear regression of dP/dt versus Left Ventricular Pressure (P): $dP/dt=(-1/\tau)*P$.

Two axis formed by the ultrasonic crystals were used to measure the segmental length of the non ischemic zone (L_{NZ}) and the ischemic zone (L_{IZ}) at end-diastole ($L_{NZ}D$ and LI_ZD) and end-systole ($L_{NZ}S$ and $L_{IZ}S$) (Figure 5.1). The Regional Passive diastolic left ventricular stiffness or myocardial stiffness was defined for each zone X as the β_X index in the relationship $LVP=b0+b1*\exp^{\beta_X L_X}$. The regional Preload Recruitable Stroke Work (rPRSW) was defined for each zone X as the slope relating Ew and L_XD in the equation: $Ew=rPRSW_X*(L_XD-L_{X0})$ were L_{X0} is the x-intercept. Both β_X and $rPRSW_X$ were calculated by regression based on the Pressure-lenght loops recorded during acute occlusion of the caudal vena cava.

iii. Microsphere study

Five mL of a 0.02% Tween 80 solution was slowly injected after collection of the hemodynamic data. Five minutes after Tween 80 injection, colored Microspheres (Dye-Trak® Triton Technology, San Diego, USA) were injected in the left atrium through the 18 Gauge catheter. Different colors of microspheres were used for baseline and ischemia. Ten seconds after injection, an aortic blood sample was drawn through the 16 Gauge catheter at a constant rate of 10 mL/min in a 35cc syringe. The hearts were harvested during necropsy in order to verify the positioning of the sutures and to obtain myocardial tissue samples from the Non Ischemic Zone (NIZ) and the Ischemic Zone (IZ) (Figure 5.1).

Following tissue digestion or blood hemolysis, the microspheres were recovered by sedimentation[9] and regional blood flow of the myocardium was calculated.[10]

iv. Statistical analysis.

The data was analyzed using a statistical software (JMP, SAS Institute Inc, Cary, USA). For each hemodynamic and energetic parameter, a One-Way Analysis of Variance for repeated measurements was used to assess the time effect. A One-Way Analysis of Variance for repeated measurements was used to compare the myocardial perfusion of the Non-Ischemic and the Ischemic Zone at baseline and after induction of ischemia. The level of significance was set at $p<0.05$.

3. Results

Six sheep were entered in the study. Coronary ligation was performed at the level of OM2 and OM3 (Figure 5.1). The positioning of the sutures was confirmed at necropsy for all the animals. An ischemic zone (IZ) was induced with a significant reduction of blood flow from 1.53 ± 0.81 mL/g/min to 0.37 ± 0.37 mL/g/min ($p=0.022$). The blood flow

in the Non-Ischemic Zone (NIZ) of the myocardium was not significantly affected from 1.65 ± 0.90 mL/g/min to 1.84 ± 0.87 mL/g/min (p=0.079)(Figure 5.2).

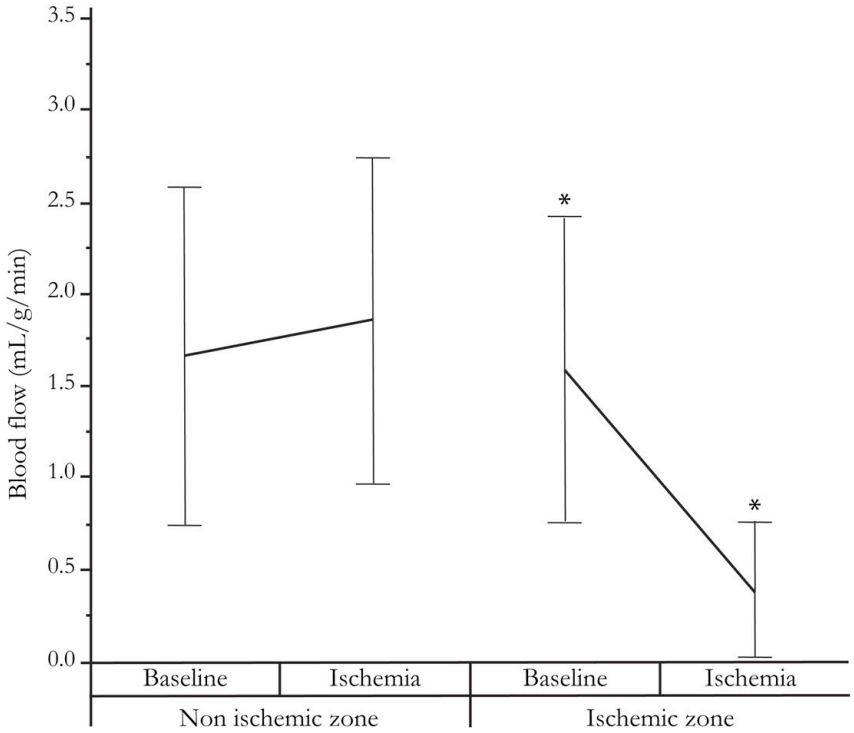

Figure 5.2: Regional blood flows of the ischemic and non ischemic zone at baseline and during ischemia. *: p<0.05.

Hemodynamic parameters collected at baseline and after ischemia are reported in Table 5.1. Left Ventricular End-Systolic Pressure decreased from 105.0 ± 12.4 mmHg at baseline to 88.7 ± 7.3 mmHg (p=0.016) at t + 5-10 min, while Left Ventricular End-Systolic Volume increased from 194.5 ± 86.9 mL at baseline to 210.5 ± 94.1 mL (p=0.039) at t + 5-10 min. Aortic Diastolic pressure decreased from 89.8 ± 10.2 mmHg at baseline to 77.7 ± 6.6 mmHg at t + 5-10 min (p=0.042). Aortic systolic pressure was decreased from 105.0 ± 13.6 mmHg at baseline to 88.0 ± 7.8 mmHg at t + 5-10 min (p=0.020) and then increased to 125.5 ± 32.4 mmHg at t + 60 min (p=0.028 when compared to t + 5-10 min).

	Baseline	t + 5-10 min	t + 60 min
HR (bpm)	93 ± 13	93 ± 8	93 ± 12
LVESP (mmHg)	105.0 ± 12.4[a]	88.7 ± 7.3[a]	94.4 ± 12.1
LVEDP (mmHg)	14.0 ± 2.0	14.6 ± 5.4	13.6 ± 5.1
ASP (mmHg)	105.0 ± 13.6[a]	88.0 ± 7.8[a,b]	125.5 ± 32.4[b]
ADP (mmHg)	89.8 ± 10.2[a]	77.7 ± 6.6[a]	82.2 ± 11.2
LVESV (mL)	194.5 ± 86.9[a]	210.5 ± 94.1[a]	208 ± 86.4
LVEDV (mL)	238.6 ± 88.1	248.9 ± 95.4	249.6 ± 90.4
SV (mL)	44.1 ± 7.4	38.4 ± 8.0	41.6 ± 9.1
dP/dt max ($mmHg.L^{-1}$)	1274 ± 381[a]	1008 ± 171[a]	1155 ± 278
Emax ($L.mmHg^{-1}$)	1.33 ± 0.47	1.23 ± 0.62	1.62 ± 0.12
τ (sec^{-1})	0.047 ± 0.006	0.051 ± 0.005	0.052 ± 0.008
β (mL^{-1})	0.351 ± 0.252	0.399 ± 0.495	0.325 ± 0.350
EDPVR Slope ($mmHg.mL^{-1}$)	0.017 ± 0.01	0.019 ± 0.01	0.018 ± 0.01
PRSW (mmHg)	60.7 ± 9.1[a]	50.0 ± 15.4	42.3 ± 4.3[a]
PVA (mmHg.L)	6260 ± 1387[a,b]	4149 ± 1299[a]	4368 ± 1632[b]
Ew (mmHg.L)	3877 ± 1287[a,b]	2334 ± 872[a]	2507 ± 883[b]

Table 5.1: HR: Heart Rate, LVESP: Left Ventricular End-Systolic Pressure, LVEDP: Left Ventricular end-Diastolic Pressure, ASP: Aortic Systolic Pressure, ADP: Aortic Diastolic Pressure, LVESV: Left Ventricular End-Systolic Volume, LVEDV: Left Ventricular End-Diastolic Volume, dP/dt max: Mean maximum value of the derivative of left ventricular pressure against time, Emax: Maximum elastance of the left ventricle, τ: Isovolumetric relaxation time constant, β: Passive diastolic left ventricular stiffness, PRSW: Global Preload Recruitable Stroke Work, rPRSWIZ: Regional Preload Recruitable Stroke Work of the ischemic zone, rPRSWNIZ: Regional Preload Recruitable Stroke Work of the non ischemic zone, PVA: Pressure-Volume Area, Ew: Stroke work of the left ventricle.
Values with a similar superscript letter are significantly different ($p<0.05$).

Ischemia reduced PRSW from 60.7 ± 9.1 mmHg at baseline to 42.3 ± 4.3 mmHg at t + 60 min (p=0.002). The regional Preload Recruitable Stroke Work of the Non Ischemic Zone ($rPRSWN_{IZ}$) was 51.6 ± 11.8 $mmHg.L.m^{-1}$ at baseline, 55.2 ± 16.4 $mmHg.L.m^{-1}$ at t+5-10 min (p=0.603) and 53.3 ± 14.1 $mmHg.L.m^{-1}$ at t + 60 min (p=0.836). The regional Preload Recruitable Stroke Work for ischemic zone ($rPRSW_{IZ}$)

decreased from 96.2 ± 33.9 mmHg.L.m^{-1} at baseline to 59.2 ± 28.6 mmHg.L.m^{-1} at t + 5-10 min (p=0.026) and to 63.7 ± 25.7 mmHg.L.m^{-1} for t + 60 min (p=0.032 when compared to baseline).

Emax was not affected by ischemia (p=0.353) with V_0 increasing from 141.6 ± 70.8 mL at baseline to 149.4 ± 72.8 ml at t + 5-10 min (p=0.447) and to 159.0 ± 67.0 mL

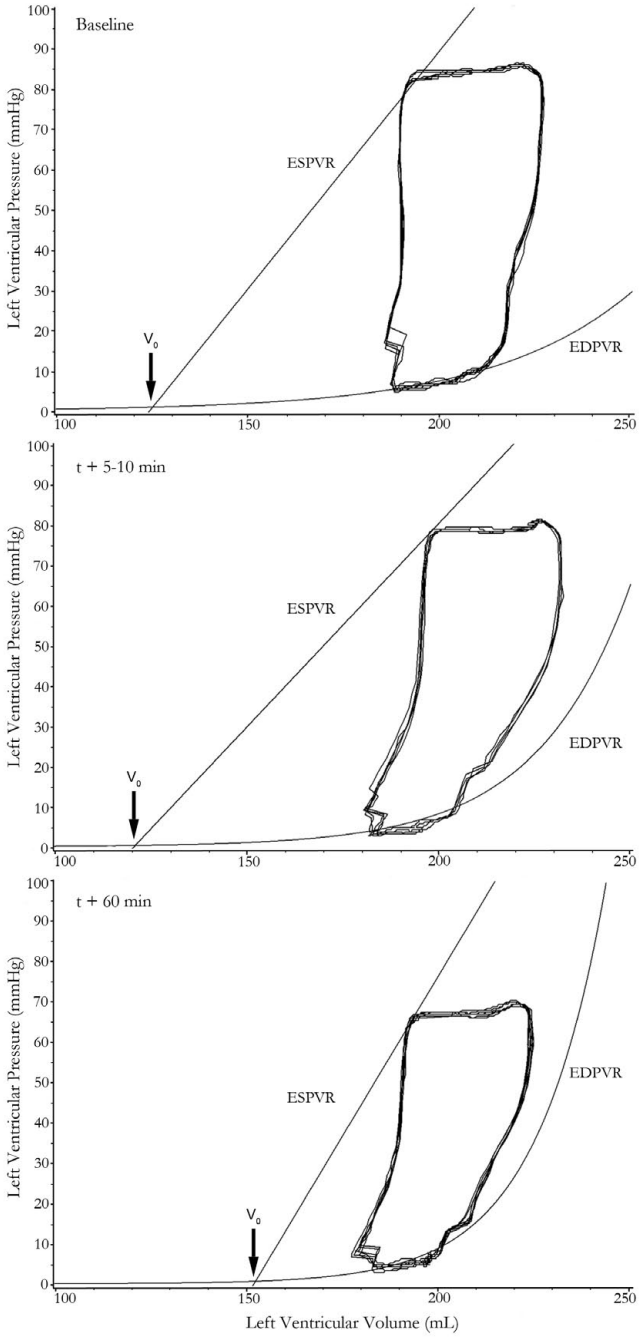

Figure 5.3: Pressure-Volume loops of five consecutive cardiac cycles representative of a stable hemodynamic state at baseline (top), t + 5-10 min (middle) and t + 60 min (bottom). ESPVR: End-Systolic Pressure-Volume Relationship, V_0: volume intercept of the ESPVR, EDPVR: End-Diastolic Pressure-Volume Relationship.

at t + 60 min (P=0.0043) (Figure 5.3) while dP/dt decreased from 1274 ± 381 mmHg.L-1 at baseline to 1008 ± 171 mmHg.L-1 at t + 5-10 min (p=0.044).

The Mitral Regurgitant volume was 1.2 ± 2.3 mL at baseline, -1.3 ± 1.6 mL at t + 5-10 min and 0.2 ± 0.5 mL at t + 60 min (p=0.746).

Passive diastolic stiffness of the left ventricle β (p=0.059) and the index of isovolumetric relaxation τ (p=0.599) remained unchanged after induction of regional ischemia. The slope of EDPVR was not affected by induction of ischemia at t + 5-10 min

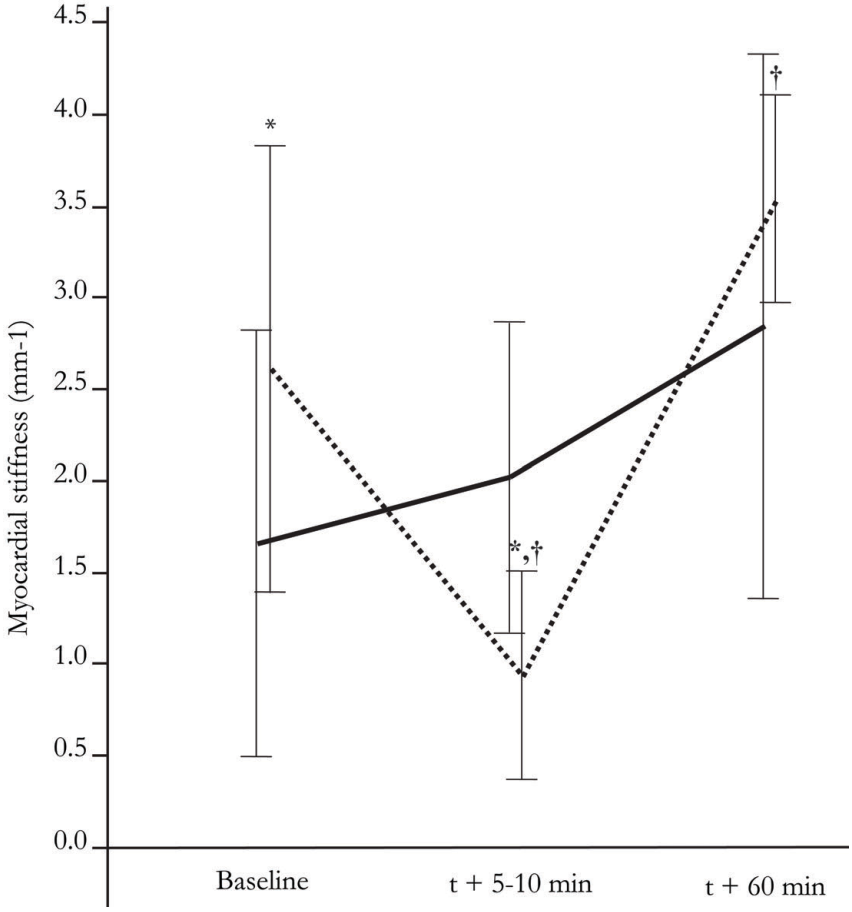

Figure 5.4: Passive regional left ventricular stiffness of the ischemic (dash line) and non ischemic (solid line) zones at baseline, t + 5-10 min and t + 60 min. * and †: p<0.05.

(p=0.488) and t + 60 min (p=0.707). Myocardial stiffness of the Non Ischemic Zone (β_{NIZ}) was 1.70 ± 1.10 mm-1 at baseline, 2.00 ± 1.30 mm-1 at t + 5-10 min (p=0.64) and 2.90

± 1.50 mm-1 t + 60 min (p=0.19). Myocardial stiffness of the Ischemic Zone (β_{IZ}) decreased from 2.63 ± 1.23 mm-1 at baseline to 0.94 ± 0.57 mm-1 at t + 5-10 min (p=0.014). At t + 60 min β_{IZ} was 3.56 ± 0.57 mm-1 which was significantly increased when compared to t+5-10 min (p=0.033) but not when compared to baseline (p=0.376) (Figure 5.4).

The total mechanical energy (PVA) decreased after induction of ischemia from 6260 ± 1387 mmHg.L at baseline to 4149 ± 1299 mmHg.L at t + 5-10 min (p=0.019). After one hour of ischemia, PVA remained significantly lower at 4368 ± 1632 mmHg.L than at baseline (p<0.001). The stroke work developed by the left ventricle (EW) described a similar evolution with a decrease from a baseline value of 3877 ± 1287 mmHg.L to 2334 ± 872 mmHg.L at t + 5-10 min (p=0.037). EW stayed below the baseline level for t + 60 min at 2507 ± 883 mmHg.L (p=0.013). Contractile efficiency (CE) was not significantly reduced from 61 ± 12% at baseline to 56 ± 9% at t + 5-10 min and 59 ± 6% at t + 60 min (p=0.513) by the acute regional ischemia.

The segmental length of the non ischemic zone (L_{NZ}) remained unchanged with ischemia (table 5.2). The segmental length of the ischemic zone (L_{IZ}) increased at end-systole from 65.8 ± 12.3 mm at baseline to 69.5 ± 14.0 mm at t + 60 min (p=0.025) but did not change at end-diastole.

		Baseline	t + 5-10 min	t + 60 min
L_{NZ} (mm)	D	85.9 ± 21.0	87.9 ± 22.9	86.2 ± 20.5
	S	77.4 ± 19.1	80.7 ± 21.3	78.2 ± 18.8
L_{IZ} (mm)	D	71.1 ± 14.12	71.42 ± 15.8	71.7 ± 14.7
	S	65.8 ± 12.3[a]	66.7 ± 13.2	69.5 ± 14.0[a]

Table 5.2: L_{NZ}: Segmental length of the non ischemic zone, L_{IZ} : Segmental length of the ischemic zone, D: End-diastole, S: End-Systole. Values with a similar superscript letter are significantly different (p<0.05).

4. Discussion

Acute myocardial ischemia of the posterior papillary muscle did not induce mitral valve regurgitation in sheep but induced a reversible reduction of regional passive diastolic stiffness of the ischemic zone of the left ventricle. Within an hour after induction of ischemia the compliance of the ischemic zone was similar to baseline. The overall left ventricular passive compliance was not affected by ischemia. In this study, we have characterized the evolution of a regional acute posterolateral myocardial ischemia and its impact on the hemodynamic and energetic state of the left ventricle.

The coronary circulation in sheep is very similar to human, making it a valuable large animal model to assess the impact of acute myocardial ischemia on systolic and diastolic left ventricular function[11] Although several large animal models of acute myocardial infarction have been described,[11-14] none investigates the very early stage of left ventricular remodeling and both global and regional responses to acute regional myocardial infarction.

Ligating the second and third obtuse marginal branches of the left circumflex coronary artery induced consistently an infarcted area involving 21% of the posterolateral aspect of the left ventricle including the posterior papillary muscle.[11] The ischemic zone created was well demarcated in all sheep with a significantly decreased coronary blood flow. The absence of collateral coronary circulation in sheep[15] allowed us to define specific myocardial regions, with or without ischemia.

Discoloration of the myocardium was visible immediately after occlusion the two obtuse branches and remained visible during the entire experiment. Regional myocardial ischemia induced mild hemodynamic changes. Preload recruitable stroke work, PVA and

external work were significantly reduced after induction of the infarction. Aortic systolic pressure was significantly reduced. Mitral regurgitation was absent at each time point. Since the occlusion of those two obtuse branches should affect only 21% of the left ventricular wall left ventricular pressures and volumes were not significantly affected 60 minutes after the induction of ischemia. The first derivative of the left ventricular pressure against time was significantly reduced at t + 5-10 min only, while Emax was not affected. As opposed to dP/dt, Emax is not load sensitive. Reduced PVA associated with a conserved Emax implies a parallel shift to the right of ESPVR with an augmentation of Vo due to the dilation of the left ventricle in diastole and systole. The ischemic segment has a significant augmentation in length at t + 60 min in systole.

Diastolic dysfunction of the entire left ventricle was not affected. The constant of isovolumetric relaxation time, the slope of End Diastolic Pressure Volume Relationship and the index of passive left ventricular stiffness were not affected by the infarction. However when we analyzed the passive stiffness of the ischemic and the non ischemic area of the left ventricular wall the passive stiffness of the ischemic area was reduced during the first 10 minutes but returned to normal one hour after induction of ischemia. The index of left ventricular diastolic stiffness is usually affected by chronic changes in the left ventricular wall after ischemia like fibrosis or extracellular matrix remodeling. In an acute situation the collagen matrix was not altered. This increase in compliance can be due to initial slippage of myocytes, edema, decrease wall thickness, coronary artery turgor, or abnormality of calcium handling by the sarcoplasmic reticulum.[16, 17, 18, 19] Abnormal calcium handling is mostly affecting inactivation phase of relaxation,[17] however we were unable to detect a delayed relaxation phase in our study. Perhaps infarct size may have been too small to detect a global ventricular effect. Decreased ventricular wall thickness due to vascular collapse could have been responsible for the

early increased compliance according to the Salisbury effect.[20] Olsen et al.[19] showed that coronary pressure is an independent determinant of ventricular compliance, hence acute ligation of coronary arteries may explain the observed early increase compliance. Preload recruitable stroke work was significantly decreased for the area of infarction which demonstrates an abnormal contractile function of this area of the myocardium, which might be another indicator of abnormal calcium handling. Three dimensional echocardiography has shown a reduction of left ventricular thickness associated with passive stretching.[21, 22] Paradoxical motion of the ischemic zone during systole could also induce significant dilation of the ischemic zone and contribute to the increase compliance of that segment of the left ventricular wall. However, the length of the ischemic segment was significantly increased only in systole 60 min after induction of ischemia therefore bulging of the ischemic zone may not be the major cause of the modification of compliance in the early phase. The late increase in ischemic myocardial stiffness that we observed at t + 60 min can be due to abnormal calcium handling by the sarcoplasmic reticulum resulting in cytoplasmic calcium overload. Varma et al.[23] showed that calcium overload in the cytoplasm can alter the compliance of the left ventricle because it altered actin-myosin interaction.

Regional preload recruitable stroke work of the ischemic zone was depressed immediately after induction of the infarction and persisted at t + 60 min, indicating reduction of contractile function of this zone. This effect has been previously reported in rat,[24, 25] dog[26, 27] and swine[28] models. This regional adaptation had a repercussion on the overall left ventricle mechanical work (EW) without a compensatory mechanism from the non–ischemic zone of the left ventricle. Since PVA and EW were reduced without an effect on contractile efficiency, contractility of the entire left ventricle was reduced. The non-ischemic myocardium is not compensating for the ischemic zone since preload

recruitable stroke work of this non ischemic zone is not increasing and PVA is not increasing either. The augmentation of afterload related to the dilation of the ischemic zone was not sufficient to decrease contractile efficiency.

5. Conclusions

A mild acute posterolateral myocardial infarction induced early systolic and diastolic regional dysfunction. Regional ischemia immediately altered global left ventricular function but changes were not seen in diastolic function. No mitral regurgitation was identified. The infarction most likely increased in size and the non ischemic myocardium did not compensate for the left ventricular remodeling. Both systolic and diastolic functions were most likely related to the same cellular mechanism.

6. References

1. Richards AM, Nicholls MG, Espiner EA, Lainchbury JG, Troughton RW, Elliott J, Frampton C, Turner J, Crozier IG, Yandle TG. B-type natriuretic peptides and ejection fraction for prognosis after myocardial infarction. Circulation. 2003;107(22):2786-2792.

2. Berning J, Steensgaard-Hansen F. Early estimation of risk by echocardiographic determination of wall motion index in an unselected population with acute myocardial infarction. Am J Cardiol. 1990;65(9):567-576.

3. Thune JJ, Kober L, Pfeffer MA, Skali H, Anavekar NS, Bourgoun M, Ghali JK, Arnold JM, Velazquez EJ, Solomon SD. Comparison of regional versus global assessment of left ventricular function in patients with left ventricular dysfunction, heart failure, or both after myocardial infarction: the valsartan in acute myocardial infarction echocardiographic study. J Am Soc Echocardiogr. 2006;19(12):1462-1465.

4. Lopes LR, Joao I, Vinhas H, Simoes O, Cotrim C, Catarino C, Carrageta M. Evaluation of systolic and systo-diastolic function: the Tei index in acute myocardial infarction treated with acute reperfusion therapy--early and late evaluation. Rev Port Cardiol. 2007;26(6): 649-656.

5. Glower DD, Schaper J, Kabas JS, Hoffmeister HM, Schaper W, Spratt JA, Davis JW, Rankin JS. Relation between reversal of diastolic creep and recovery of systolic function after ischemic myocardial injury in conscious dogs. Circ Res. 1987;60(6):850-860.

6. Husic M, Norager B, Egstrup K, Moller JE. Serial changes in regional diastolic left ventricular function after a first acute myocardial infraction. J Am Soc Echocardiogr. 2005;18(11):1173-1180.

7. DeKeulenaer GW, Brutsaert DL. Molecular Mechanisms of Diastolic Dysfunction. In: Smisteh OA, Tendera M, eds. Diastolic Heart Failure. London: Springer; 2008:3-19.

8. Kitzman DW, Little WC, Brubaker PH, Anderson RT, Hundley WG, Marburger CT, Brosnihan B, Morgan TM, Stewart KP. Pathophysiological characterization of isolated diastolic heart failure in comparison to systolic heart failure. JAMA. 2002;288(17): 2144-2150.

9. Van Oosterhout MF, Willigers HM, Reneman RS, Prinzen FW. Fluorescent microspheres to measure organ perfusion: validation of a simplified sample processing technique. Am J Physiol. 1995;269(2 Pt 2):H725-733.

10. Kowallik P, Schulz R, Guth BD, Schade A, Paffhausen W, Gross R, Heusch G. Measurement of regional myocardial blood flow with multiple colored microspheres. Circulation. 1991;83(3):974-982.

11. Llaneras MR, Nance ML, Streicher JT, Lima JA, Savino JS, Bogen DK, Deac RF, Ratcliffe MB, Edmunds LH, Jr. Large animal model of ischemic mitral regurgitation. Ann Thorac Surg. 1994;57(2):432-439.

12. Markovitz LJ, Savage EB, Ratcliffe MB, Bavaria JE, Kreiner G, Iozzo RV, Hargrove WC, 3rd, Bogen DK, Edmunds LH, Jr. Large animal model of left ventricular aneurysm. Ann Thorac Surg. 1989;48(6):838-845.

13. Moainie SL, Gorman JH, 3rd, Guy TS, Bowen FW, 3rd, Jackson BM, Plappert T, Narula N, St John-Sutton MG, Narula J, Edmunds LH, Jr., Gorman RC. An ovine model of postinfarction dilated cardiomyopathy. Ann Thorac Surg. 2002;74(3):753-760.

14. Pfeffer MA, Braunwald E. Ventricular remodeling after myocardial infarction. Experimental observations and clinical implications. Circulation. 1990;81(4):1161-1172.

15. Schaper W, Flameng W, De Brabander M. Comparative aspects of coronary collateral circulation. Adv Exp Med Biol. 1972;22:267-276.

16. Buja LM, McAllister JHA. Coronary Artery Disease: Pathologic Anatomy and Pathogenesis. In: Willerson JT, Wellens HJJ, Cohn JN, Holmes JDR, eds. Cardiovascular Medicine. London: Springer; 2007:593-607.

17. Gillebert TC, Leite-Moreira AF. Pathophysiologic Aspects of Myocardial Relaxation and End-Diastolic Stiffness of Cardiac Ventricles In: Smisteh OA, Tendera M, eds. Diastolic Heart Failure. London: Springer; 2008:21-39.

18. Zile MR, Brutsaert DL. New concepts in diastolic dysfunction and diastolic heart failure: Part I: diagnosis, prognosis, and measurements of diastolic function. Circulation. 2002;105(11):1387-1393.

19. Olsen CO, Attarian DE, Jones RN, Hill RC, Sink JD, Lee KL, Wechsler AS. The coronary pressure-flow determinants left ventricular compliance in dogs. Circ Res. 1981;49(4): 856-865.

20. Salisbury PF, Cross CE, Rieben PA. Influence of coronary artery pressure upon myocardial elasticity. Circ Res. 1960;8:794-800.

21. Jackson BM, Parish LM, Gorman JH, 3rd, Enomoto Y, Sakamoto H, Plappert T, St John Sutton MG, Salgo I, Gorman RC. Borderzone geometry after acute myocardial infarction: a three-dimensional contrast enhanced echocardiographic study. Ann Thorac Surg. 2005;80(6):2250-2255.

22. Messas E, Guerrero JL, Handschumacher MD, Chow CM, Sullivan S, Schwammenthal E, Levine RA. Paradoxic decrease in ischemic mitral regurgitation with papillary muscle dysfunction: insights from three-dimensional and contrast echocardiography with strain rate measurement. Circulation. 2001;104(16):1952-1957.

23. Varma N, Morgan JP, Apstein CS. Mechanisms underlying ischemic diastolic dysfunction: relation between rigor, calcium homeostasis, and relaxation rate. Am J Physiol Heart Circ Physiol. 2003;284(3):H758-771.

24. He MX, Downey HF. Downregulation of ventricular contractile function during early ischemia is flow but not pressure dependent. Am J Physiol. 1998;275(5 Pt 2):H1520-1523.

25. Galinanes M, Hearse DJ, Shattock MJ. The role of the rate of vascular collapse in ischemia-induced acute contractile failure and decreased diastolic stiffness. J Mol Cell Cardiol. 1996;28(3):519-529.

26. Glower DD, Spratt JA, Kabas JS, Davis JW, Rankin JS. Quantification of regional myocardial dysfunction after acute ischemic injury. Am J Physiol. 1988;255(1 Pt 2):H85-93.

27. Pirzada FA, Ekong EA, Vokonas PS, Apstein CS, Hood WB, Jr. Experimental myocardial infarction. XIII. Sequential changes in left ventricular pressure-length relationships in the acute phase. Circulation. 1976;53(6):970-975.

28. Guth BD, Schulz R, Heusch G. Time course and mechanisms of contractile dysfunction during acute myocardial ischemia. Circulation. 1993;87(5 Suppl):IV35-42.

Chapter VI
Correction of Acute Functional Mitral Regurgitation: development of e New Epicardial device

Current proposed therapies for functional mitral regurgitation (FMR) have the goals of correcting the valvular geometry and structural stabilization of the valvular-ventricular complex. While the presence of an external constraint appears to be crucial in controlling or reversing the progression of the left ventricular remodeling,[1-3] modification of the mitral valve apparatus is considered as critical in the correction of FMR.[4] Undersized annuloplasty restores annular shape and reduces the septolateral dimension of the mitral valve,[5] and hence could be considered as a focal constraint. Although the subvalvular changes are partially addressed,[6] the ventricular remodeling can progress and may lead to the recurrence of FMR.[7,8] Recent studies emphasize the importance of restoring the structural organization of the valve apparatus.[9,10] Correction of the papillary muscle tethering can be achieved directly by cordal cutting[11] or translocation,[12] papillary muscle approximation[13] or relocation,[14] or indirectly by applying an external force to the papillary muscles.[15]

The Coapsys (Myocor, Maple Grove, Minnesota, USA) device has been shown to reduce functional mitral regurgitation, however part of the device is in contact with the

blood, which can increase the risk of thromboembolism in the long term. Polymer injection in the ventricular wall in close proximity to the papillary muscles has been described recently as an alternative method for papillary repositioning and acute correction of FMR.[16,17] Long-term effect of the polymer injection within the myocardium is unknown.

1. Hypothesis

The purpose of this study was to evaluate an epicardial device designed to displace the papillary muscles toward a more normal position. The effects of the device on functional mitral regurgitation, mitral annulus diameter and diastolic function in an acute sheep model of functional mitral valve regurgitation were evaluated.

2. Material and methods

The experimental protocol used for this investigation received the approval of the Animal Care and Use Committee (#: 07-003A-01) of the Colorado State University (Fort Collins, CO, USA).

i. Surgical preparation

Seven adult female Dorsett sheep were premedicated with diazepam (7.5 mg IV) and induced with ketamine (250 mg IV). After endotracheal intubation, they were ventilated and maintained under anesthesia with continuous administration of Isoflurane (1.5 to 3%). Fentanyl (20 µg/kg/h IV) and Lidocaine (100 mg/kg/min IV) were continually infused. Left chest-wall resection and subtotal pericardectomy were performed.

An ultrasonic flow probe was placed around the ascending aorta (Transonic® Flow probe, Transonic Systems Inc., NY, USA). A high fidelity microtip pressure catheter with two pressure sensors (Pressure Mikro-Tip®, Millar instruments Inc., Houston, USA) was inserted in the left ventricle and proximal aorta through an incision at the apex of the

heart. An 18 Gauge catheter was inserted in the left atrium and connected to a fluid filled pressure transducer. Four 2 mm ultrasonic crystals (SonometricsCorp., London, Canada) were implanted in the epicardium to measure the major and minor axis of the left ventricle. The minor axis is defined between the left anterior descending coronary artery and the left posterior descending coronary artery, distal to the coronary sinus. The minor axis was also used as a measurement for the anteroposterior diameter of the annulus. Descending aorta was dissected and a curved vascular clamp was pre-placed for aortic banding. The brachiocephalic trunk was dissected and a Rummel tourniquet was pre-placed. The caudal vena cava was exposed and a Rummel tourniquet was placed.

ii. Induction of acute functional mitral regurgitation with aortic banding

Aortic banding was induced with complete occlusion of the descending aorta and partial occlusion of the brachiocephalic trunk until an aortic blood flow of 0.8 $L.min^{-1}$ was reached. To be able to repeat the occlusion and the degree of aortic banding between the device “on” and “off” only the aortic clamp was released and replaced when needed.

iii. Application of the external device

An external device (Figure 6.1 and 6.2) was pre-placed on the epicardium with four mattress sutures mounted on Rummel tourniquet. The device was positionned on the left ventricle to have the two pads pushing on the papillary muscle in an apico-basal direction toward the center of the annulus. Then four mattress sutures mounted on Rummel tourniquet were placed to stabilized the device in the desire position. Two proximal mattress sutures were placed close to the annulus sparing the coronary arteries and two sutures were also placed close to the apex. None of the sutures were interfering with coronary arteries. The crossbar was then placed to connect the two vertical legs of the device. Sutures were maintained loose for the recording of data with

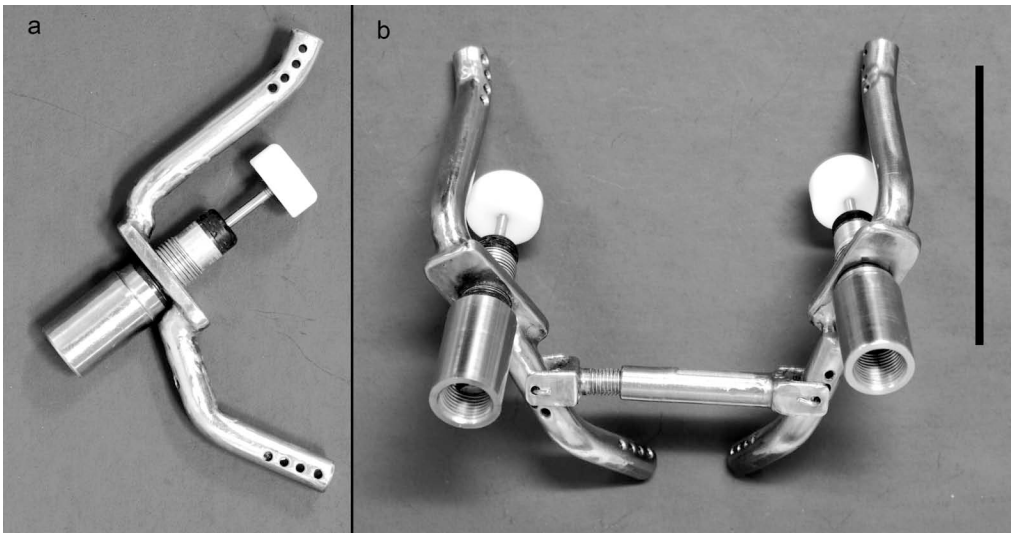

Figure 6.1: Epicardial device. a: one vertical leg with annular and apical fixation points (white arrows) to place mattress sutures, the pad is position at the level of the papillary muscles. b: The connecting bar has been placed between the two vertical legs to complete the device.

the device “off”. The sutures were tightened to apply the device for the recording of the

data with the device “on”.

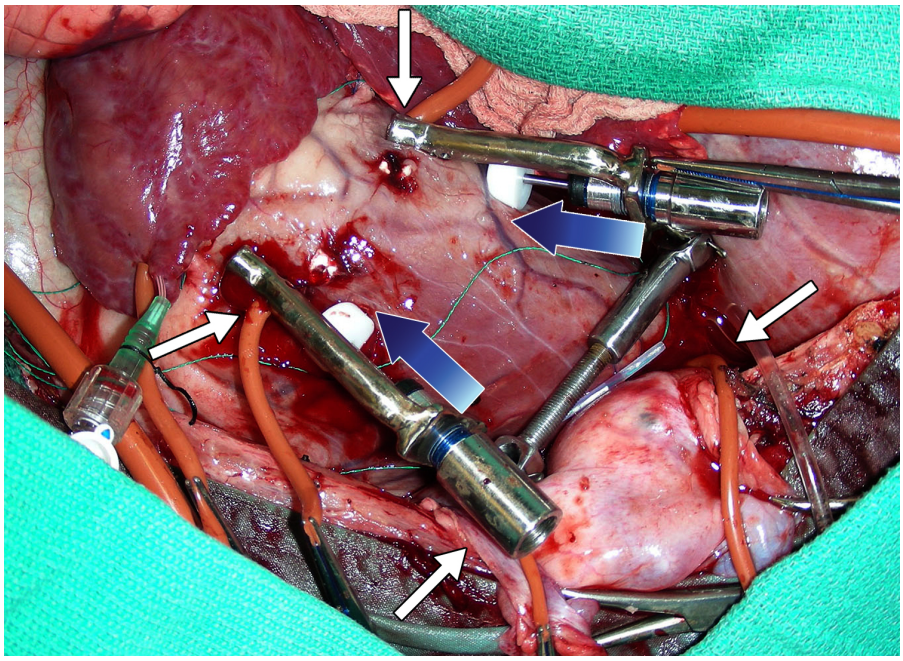

Figure 6.2: The device was placed to have the two pads pushing on the papillary muscles in an apicobasal direction toward the center of the annulus (blue arrows). The four sutures holding the device on the epicardium (white arrows) were maintained loose for the recording of data with the device “off”. The sutures were tightened to apply the device for the recording of the data with the device “on”.

iv. Data acquisition

Data were recorded by a data acquisition system (Sonolab and Sonosoft, SonometricsCorp., London, Canada). Data were recoded at baseline, after induction of aortic banding with the device “on” or “off” according to the protocol one or two (Figure 2.3). In half of the sheep, data were first recoded with device “on” and in the other half the data were recoded with the device “off” first. Data was collected for at least three minutes until the left atrial, left ventricular pressure, and aortic flow were stable. Then only, aortic clamp was released for five minutes and after return to baseline value for left ventricular pressure and aortic flow. The experiment was repeated with either the device on or off according to the protocol (Figure 6.3). At baseline the vena cava was gradually

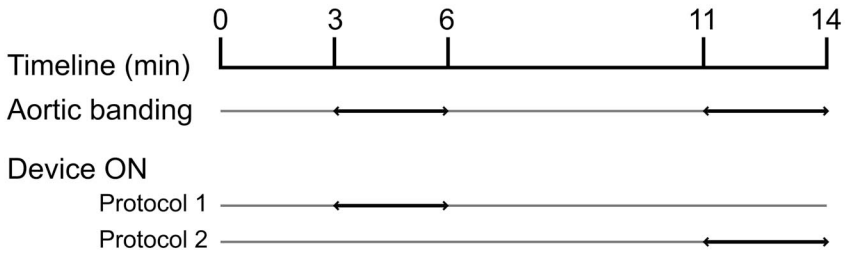

Figure 6.3: Data were recorded at baseline, after induction of aortic banding with the device “on” or “off” according to the protocol. In half of the sheep, data were first recorded with device “on” and in the other half the data were recoded with the device “off” first. Data was collected for at least 3 min until the left atrial, left ventricular pressures, and aortic flow were stable

occluded in order to calculate EDPVR (End-Diastolic Pressure Volume Relationship) and ESPVR (End-Systolic Pressure Volume Relationship) by linear regression. At the end of the experiment, the animals were euthanized by injection of 20 mL of pentobarbital IV. The hearts were harvested during necropsy in order to verify the positioning of the device.

Data were later analyzed by data analysis software (Cardiosoft, SonometricsCorp., London, Canada). The heart rate was calculated based on the recorded electrocardiogram. End-Systolic Left Ventricular Pressure (ESLVP), End-Diastolic Left Ventricular Pressure (EDLVP), Aortic Diastolic Pressure (ADP), Aortic Systolic Pressure (ASP) and Mean Aortic Pressure (MAP) were recorded with the Millar catheter. Mean Left Atrial Pressure (MLAP) was recorded through the 18 Gauge atrial catheter. Aortic Blood Flow was recorded *via* the aortic ultrasonic flow probe. End-Diastolic Left Ventricular Volume (EDLVV) and End-Systolic Left Ventricular Volume (ESLVV) were calculated based on the ultrasonic crystals calculations using an ellipsoid model. We used the minor axis of the left ventricle to measure the anterior-posterior annulus diameter. The first derivative of left ventricle pressure curve against time was used to determine dP/dt max and dP/dt min. The first derivative of left ventricle volume curve against time was used to determine dV/dt min. External work (EW) of the left ventricle was the area of the Pressure-Volume loop. Left ventricle Stroke Volume (SV) was calculated based on the difference between End-Diastolic Left Ventricular Volume and End-Systolic Left Ventricular Volume. Aortic Stroke Volume (ASV) was obtained by dividing the mean aortic blood flow by the heart rate. Mitral Regurgitant Volume was then defined as: MRV=SV-ASV. Passive diastolic left ventricular stiffness was defined as the β index in the relationship $LVP=b_0+b_1*\exp(\beta*LVV)$. The left ventricular exponential time constant of isovolumic relaxation τ was calculated by performing a linear regression of dP/dT versus Left Ventricular Pressure (P): $dP/dT= (-1/\tau)*P$.

v. Statistical analysis

The data was analyzed using a statistical software (JMP, SAS Institute Inc, Cary, USA). Hemodynamic parameters with device on and off were compared between protocol 1 and 2 with a paired-t test. Hemodynamic parameters (baseline vs aortic

banding, and device “on” vs “off” during aortic banding) were compared with a paired-t test. The level of significance was set at $p<0.05$.

3. Results

Seven adult sheep weighting from 55 to 75 kg were studied. Hemodynamic parameters collected at baseline are reported in Table 6.1.

Parameter	Baseline
HR (bpm)	88 ± 12
EDLVP (mm Hg)	16.1 ± 3.4
ESLVP (mm Hg)	105.1 ± 6.3
MLAP (mm Hg)	9.7 ± 5.8
ADP (mm Hg)	92.1 ± 8.3
ASP (mm Hg)	106.0 ± 7.5
MAP (mm Hg)	96.7 ± 7.9
ABF (L/min)	4.4 ± 0.8
EDLVV (ml)	235.9 ± 49
ESLVV (ml)	185.9 ± 41.9
DAP ann D (mm)	74.6 ± 7.8
DAP ann S (mm)	68.7 ± 7.4
SV (ml)	50.0 ± 8.6
ASV (ml)	50.6 ± 8.3
dP/dt max (mmHg.sec^{-1})	1035 ± 154
EW (ml.mmHg)	4060 ± 1175
β (ml^{-1})	0.09 ± 0.09

Table 6.1: HR: Heart Rate, EDLVP: End-Diastolic Left Ventricular Pressure, ESLVP: End-Systolic Left Ventricular Pressure, MLAP: Mean Left Atrial Pressure, ADP: Aortic Diastolic Pressure, ASP: Aortic Systolic Pressure, MAP: Mean Aortic Pressure, ABF: Aortic Blood Flow, EDLVV: End Diastolic Left Ventricular Volume, ESLVV: End Systolic Left Ventricular Volume, DAP ann D: Diameter Antero-Posterior annulus during Diastole, DAP ann S: Diameter Antero-Posterior annulus during Systole, SV: Left ventricular Stroke Volume, ASV: Aortic Stroke Volume, dP/dt max: mean maximum value of the first derivative of left ventricular pressure against time, Ew: External work of the left ventricle, β: Passive diastolic left ventricular stiffness.

i. Induction of mitral regurgitation with aortic banding

Aortic banding increased (p<0.001) left ventricular end systolic pressure from 105.1 ± 6.3 to 205.2 ± 19.5 mmHg. End diastolic pressure increased (p<0.001) from 16.1 ± 3.4 to 46.4 ± 6.6 mmHg (Figure 6.4). Index of left ventricular contractility, dP/dt max

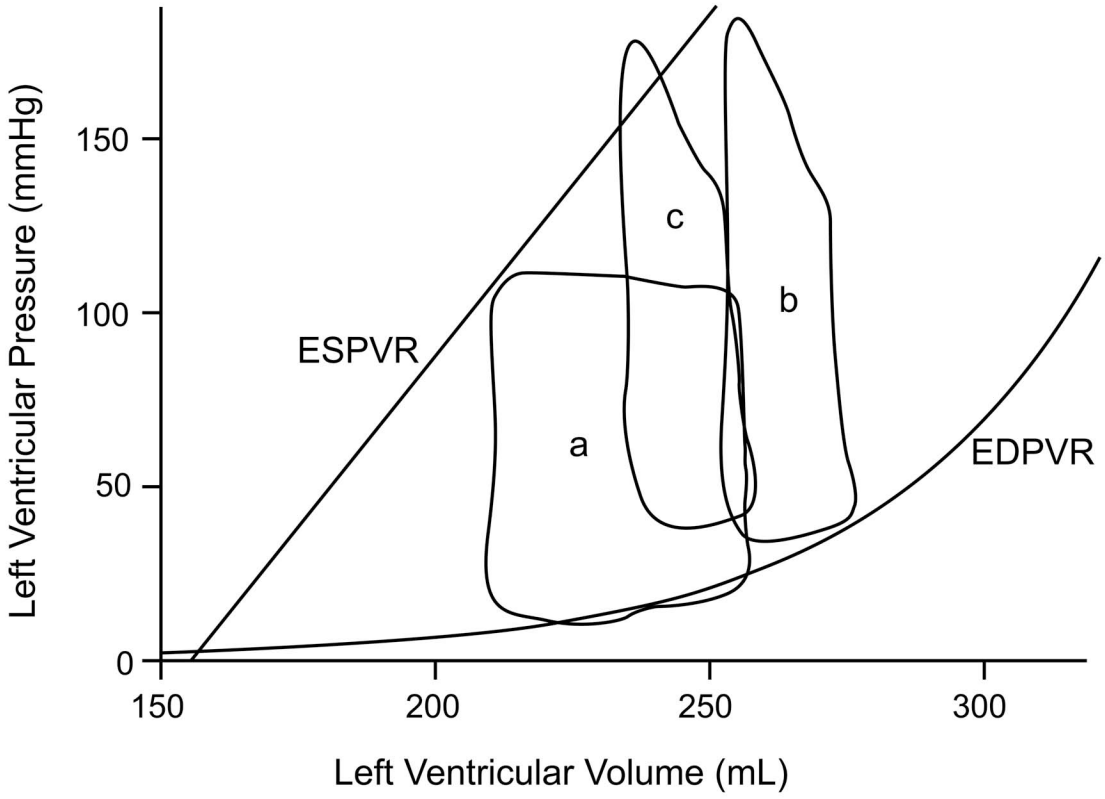

Figure 6.4: Pressure-Volume loops at baseline (a) and during aortic banding without the device (b) and with the device (c). ESPVR: End-Systolic Pressure-Volume Relationship at baseline conditions. EDPVR: End-Diastolic Pressure-Volume Relationship at baseline conditions. Each curve represents the mean trace of ten cardiac cycles with the heart in stable hemodynamic conditions.

increased (p=0.007) from 1035.40 ± 154 to 1605.10 ± 698 mmHg.s-1. End-diastolic left ventricular volume was not different (p=0.185) before (235.9 ± 49 ml) and after (241.9 ± 52.5 ml) aortic banding. End-systolic left ventricular volume increased (p<0.001) from 185.9 ± 41.9 to 219.6 ± 44.0 ml. The anterior-posterior annulus diameter increased from

74.6 ± 7.8 to 75.9 ± 7.8 mm during diastole (p=0.031) and from 68.7 ± 7.4 to 73.0 ± 7.3 mm during systole (p<0.001). Mechanical work decreased from 4060.0 ± 1175.0 to 2563.0 ± 1642.0 mL.mmHg (p=0.041). Left ventricular stroke volume decreased (p<0.001) from 50.0 ± 8.6 to 22.3 ± 12.4 mL. Aortic blood flow decreased (p<0.001) from 4.4 ± 0.8 to 0.7 ± 0.6 $L.min^{-1}$. Acute functional mitral regurgitant flow was 14.4 ± 5.4 mL after aortic banding (Figure 6.5). Passive left ventricular stiffness increased (p=0.004) from 0.10 ± 0.08 to 0.92 ± 0.5 mL-1.

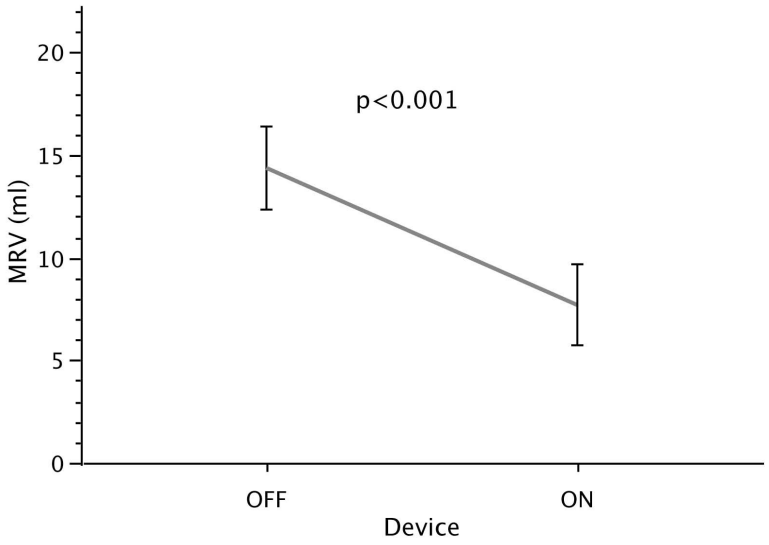

Figure 6.5: Effect of the external device on mitral regurgitant volume during aortic banding.

ii. Effect of the external device

Hemodynamic data were not significantly different between protocol 1 and protocol 2 (Table 6.2), therefore all data was pooled for further statistical analysis.

Hemodynamic parameters collected after application of the device are reported in Table 6.3, and Figure 6.4. Application of the device decreased (p=0.014) left ventricular stroke volume from 22.3 ± 12.4 mL to 18.6 ± 10.3 mL during aortic banding. Aortic stroke volume was not different (p=0.157) before (7.0 ±7.4 mL) and after (9.5 ± 6.5 mL) application of the external device.

Parameters	Protocol 1	Protocol 2	P Value
HR (bpm)	121 ± 13	101 ± 15	0.381
EDLVP (mmHg)	47.1 ± 3.6	45.5 ± 4.2	0.794
ESLVP (mmHg)	207.7 ± 10.5	201.9 ± 12.2	0.737
MLAP (mmHg)	53.8 ± 6.7	43.9 ± 6.8	0.354
ADP (mmHg)	147.3 ± 9.7	130.8 ± 11.2	0.317
ASP (mmHg)	210.1 ± 9.8	202.0 ± 11.3	0.609
MAP (mmHg)	168.2 ± 8.9	154.5 ± 10.3	0.362
ABF ($L.min^{-1}$)	0.5 ± 0.3	1.0 ± 0.3	0.234
EDLVV (mL)	226.9 ± 26.9	261.8 ± 31.0	0.434
ESLVV (mL)	209.2 ± 23.0	233.5 ± 26.6	0.519
SV (mL)	17.7 ± 6.1	28.3 ± 7.0	0.304
ASV (mL)	3.8 ± 3.4	11.3 ± 3.9	0.209
dP/dt max ($mmHg.sec^{-1}$)	1843 ± 346	1288 ± 399	0.341
dP/dt min ($mmHg.sec^{-1}$)	-1352 ± 407	-1408 ± 235	0.840
dV/dt max ($mL.sec^{-1}$)	368 ± 163	221 ± 101	0.196
EW (mL.mmHg)	1776 ± 721	3612 ± 833	0.156
β (ml^{-1})	0.97 ± 0.28	0.84 ± 0.32	0.770
τ (sec^{-1})	0.063 ± 0.020	0.066 ± 0.009	0.781

Table 6.2: HR: Heart Rate, EDLVP: End-Diastolic Left Ventricular Pressure, ESLVP: End-Systolic Left Ventricular Pressure, MLAP: Mean Left Atrial Pressure, ADP: Aortic Diastolic Pressure, ASP: Aortic Systolic Pressure, MAP: Mean Aortic Pressure, ABF: Aortic Blood Flow , EDLVV: End-Diastolic Left Ventricular Volume, ESLVV: End-Sytolic Left Ventricular Volume, SV: Stroke Volume, ASV: Aortic Stroke Volume, dP/dt max: mean maximum value of the first derivative of left ventricular pressure against time, EW: External Work, β: Passive diastolic left ventricular stiffness, τ: isovolumetric relaxation time constant.

Left ventricular end-diastolic volume decreased (p=0.044) from 241.5 ± 52.5 to 227.6 ± 46.5 mL. The external device decreased (p=0.001) acute functional mitral regurgitant flow from 14.4 ± 5.4 mL to 7.7 ± 5.2 mL (Figure 6.5). The anteroposterior diameter of the mitral annulus was not different in diastole (p=0.075) and in systole (p=0.080) after application of the device.

Passive left ventricular stiffness (β) increased (p=0.044) from 0.92 ± 0.5 to 1.18 ± 0.59 mL^{-1} after application of the device during aortic banding. Other parameters of diastolic function were not affected by the placement of the device (Table 6.3).

Parameters	Device OFF	Device ON	P Value
HR (bpm)	112 ± 26	108 ± 20	0.618
EDLVP (mmHg)	46.4 ± 6.6	50.2 ± 19.8	0.570
ESLVP (mmHg)	205.2 ± 19.5	202.8 ± 19.5	0.611
MLAP (mmHg)	48.8 ± 11.7	46.9 ± 13.9	0.537
ADP (mmHg)	140.2 ± 19.7	134.1 ± 14.2	0.108
ASP (mmHg)	207.6 ± 20.0	204.6 ± 17.8	0.300
MAP (mmHg)	162.4 ± 17.8	156.6 ± 11.3	0.137
ABF ($L.min^{-1}$)	0.7 ± 0.6	1.0 ± 0.8	0.193
EDLVV (mL)	241.5 ± 52.5	227.6 ± 46.5	0.044
ESLVV (mL)	219.6 ± 44.0	208.8 ± 38.5	0.090
DAP ann D (mm)	75.9 ± 7.8	75.5 ± 7.6	0.075
DAP ann S (mm)	73.0 ± 7.3	72.5 ± 7.3	0.080
SV (mL)	22.3 ± 12.4	18.6 ± 10.3	0.014
ASV (mL)	7.0 ± 7.4	9.5 ± 6.5	0.157
dP/dt max ($mmHg.sec^{-1}$)	1605 ± 698	1533 ± 327	0.689
dP/dt min ($mmHg.sec^{-1}$)	-1376.3 ± 319.7	-1363.40 ± 353.5	0.898
dV/dt max ($mL.sec^{-1}$)	283.6 ± 141.7	276.8 ± 160.8	0.640
EW (mL.mmHg)	2563 ± 1642	2086 ± 1146	0.065
β (ml^{-1})	0.92 ± 0.51	1.18 ± 0.59	0.044
τ (sec^{-1})	0.066 ± 0.024	0.064 ± 0.015	0.823

Table 6.3: HR: Heart Rate, EDLVP: End-Diastolic Left Ventricular Pressure, ESLVP: End-Systolic Left Ventricular Pressure, MLAP: Mean Left Atrial Pressure, ADP: Aortic Diastolic Pressure, ASP: Aortic Systolic Pressure, MAP: Mean Aortic Pressure, ABF: Aortic Blood Flow, EDLVV: End-Diastolic Left Ventricular Volume, ESLVV: End-Sytolic Left Ventricular Volume, DAP ann D: Diameter Antero-Posterior annulus during Diastole, DAP ann S: Diameter Antero-Posterior annulus during Systole, SV: Left ventricular Stroke Volume, ASV: Aortic Stroke Volume, dP/dt max: Mean maximum value of the first derivative of left ventricular pressure against time, EW: External work, β: Passive diastolic left ventricular stiffness, dP/dt min: Mean minimal value of the first derivative of left ventricular pressure against time, dV/dt max: Mean minimal value of the first derivative of left ventricular volume against time, or diastolic filling rate, τ : Active relaxation time index.

4. Discussion

Application of an epicardial device significantly reduced acute functional mitral regurgitation without affecting the anterioposterior annulus diameter and without inducing diastolic dysfunction. The augmentation of passive left ventricular stiffness did not affect the hemodynamic parameters in this animal model of functional mitral regurgitation. This device was applied on the epicardium without cardiopulmonary bypass. None of the components of the device were in direct contact with blood, which should limit the risk of thromboembolism.

Mitral regurgitation volume was reduced by 46.5%, with the application of the epicardial device. The Coapsys device reduced mitral regurgitation by 75%[18] and chordal cutting restored the baseline mitral regurgitation volume.[19] The epicardial device did not completely correct the functional mitral regurgitation for several reasons. This device works by applying pressure at the base of the papillary toward the annulus. Since our model was associated with an increased passive left ventricular stiffness, this increased stiffening more likely interfered with the effect of our device. This model was chosen because it was an acute model of functional mitral valve regurgitation with left ventricular dilatation and no anatomical modification of the mitral valve apparatus. Messas et al.[19] and Fukamachi et al.[18] used chronic models of left ventricular dilation with either coronary embolization or fast pacing, which are both associated with severe dilation of the left ventricular wall and increased compliance. With a more compliant ventricle the effect of the device should be improved because it should be able to move the papillary muscle more toward the annulus and reduce the tethering on the leaflets.

Positioning of the device is an important factor to optimize its effect. In this study we used external landmark like coronary arteries to decide how to place the device. In

the future, echocardiography would be a better tool to optimize the placement of the device. Undersized annuloplasty has been shown to significantly reduce mitral regurgitation.[20] However, while undersized annuloplasty can correct the mitral valve regurgitation and improves the geometry of the left ventricle, this technique does not address the tethering of the papillary muscle. Annuloplasty decreases the anteroposterior annulus diameter, which increases the tethering from the posterior papillary muscle. This epicardial device may be combined with a left ventricular annular procedure.[9,10,21]

Left ventricular remodeling after an ischemic event is mainly characterized by annular dilation, tethering of the papillary muscles and ventricular dysfunction.[22,23] Tethering of the papillary muscle has been proposed as the most important parameter for the development of FMR.[4,22] Functional mitral valve regurgitation was corrected in this experiment without affecting myocardial function or mitral valve annulus. Since the left ventricular end diastolic volume was significantly reduced after placement of the device, the papillary apparatus was more likely remodeled. The tethering of the mitral valve leaflet was corrected by pushing the papillary muscles toward the mitral valve leaflets.

Application of the epicardial device to the left ventricle did not interfere with diastolic function. Tau, diastolic filing rate and EDLVP were not significantly modified by the application of the epicardial device. Since the device is a rigid structure, its application increased passive left ventricular stiffness. Two sutures were placed on the anterior and posterior aspect of the mitral valve annulus. Two other sutures were at the apex of the left ventricle. As the device was maintained to the myocardium with four sutures and since the two arms of the device are only coupled by one transverse bar, the device did not interfere with the motion of the left ventricular free wall during diastole.

Furthermore, the motion of the left ventricular free wall was not limited because the device was applying pressure on two focal points in regard of the papillary muscles. Therefore, the left ventricular end diastolic volume was reduced while the left ventricular end diastolic pressure, dp/dt min, and diastolic filling rate were not affected.

In this study, supravalvular acute aortic stenosis induced functional mitral regurgitation without interfering with myocardial function. Acute augmentation of afterload resulted in a severe augmentation of left ventricular pressures, and dilation of the mitral annulus. This model induced an acute functional mitral valve regurgitation without modifying the anatomy of the mitral valve apparatus.

One limitation of our study is that we tested our device in an acute model of functional mitral valve regurgitation induced by an acute increase in afterload. The model induced a significant mitral regurgitation with an augmentation of the diameter of the annulus. However the model resulted in a significant augmentation of the left ventricular stiffness. In a more realistic chronic model of myocardial ischemia the stiffness of the left ventricle would have been decreased. Therefore, the effect would have been more important as the device works by pushing the papillary muscle toward the annulus. However, a diastolic dysfunction might have been induced because the device might have then interfered with the passive relaxation.

5. Conclusion

Application of an epicardial device designed to displace the papillary muscles decreases functional mitral valve regurgitation without interfering with diastolic function. Decreased papillary muscle tethering was the likely mechanism for correction of functional mitral regurgitation based on a decrease in end-diastolic volume and no change in anteroposterior diameter of the mitral annulus. This study did not allow

determination of whether the device is better suited to prevent or treat functional mitral valve regurgitation. This device needs to be tested with a chronic model of functional mitral regurgitation and dilation of the left ventricle. If an epicardial strategy for correction of functional mitral regurgitation proves effective, less invasive methods for device application can be envisioned.

6. References

1. Enomoto Y, Gorman JH 3rd, Moainie SL, Jackson BM, Parish LM, Plappert T et al. Early ventricular restraint after myocardial infarction: extent of the wrap determines the outcome of remodeling. Ann Thorac Surg, 2005;79:881-887.

2. Pilla JJ, Blom AS, Brockman DJ, Ferrari VA, Yuan Q, Acker MA. Passive ventricular constraint to improve left ventricular function and mechanics in an ovine model of heart failure secondary to acute myocardial infarction. J Thorac Cardiovasc Surg 2003;126:1467-1476.

3. Cheng A, Nguyen TC, Malinowski M, Langer F, Liang D, Daughters GT et al. Passive ventricular constraint prevents transmural shear strain progression in left ventricle remodeling. Circulation, 2006;114:I79-I86.

4. Otsuji Y, Handschumacher MD, Liel-Cohen N, Tanabe H, Jiang L, Schwammenthal E et al. Mechanism of ischemic mitral regurgitation with segmental left ventricular dysfunction: three-dimensional echocardiographic studies in models of acute and chronic progressive regurgitation. J Am Coll Cardiol, 2001;37:641-648.

5. Tibayan FA, Rodriguez F, Langer F, Liang D, Daughters GT, Ingels NB Jr et al. Undersized mitral annuloplasty alters left ventricular shape during acute ischemic mitral regurgitation. Circulation, 2004;110:II98-II102.

6. Timek TA, Liang D, Daughters GT, Ingels NB Jr, Miller DC. Effect of local annular interventions on annular and left ventricular geometry. Eur J Cardiothorac Surg, 2008;33:1049-1054.

7. Kuwahara E, Otsuji Y, Iguro Y, Ueno T, Zhu F, Mizukami N et al. Mechanism of recurrent/ persistent ischemic/functional mitral regurgitation in the chronic phase after surgical annuloplasty: importance of augmented posterior leaflet tethering. Circulation, 2006;114:I529-I534.

8. Gelsomino S, Lorusso R, Caciolli S, Capecchi I, Rostagno C, Chioccioli M et al. Insights on left ventricular and valvular mechanisms of recurrent ischemic mitral regurgitation after restrictive annuloplasty and coronary artery bypass grafting. J Thorac Cardiovasc Surg, 2008;136:507-518.

9. Ueno T, Sakata R, Iguro Y, Yamamoto H, Ueno M, Matsumoto K et al. Impact of subvalvular procedure for ischemic mitral regurgitation on leaflet configuration, mobility, and recurrence. Circ J, 2008;72:1737-1743.

10. Prucz RB, Weiss ES, Patel ND, Nwakanma LU, Shah AS, Conte JV. The impact of surgical ventricular restoration on mitral valve regurgitation. Ann Thorac Surg, 2008;86:726-734.

11. Borger MA, Murphy PM, Alam A, Fazel S, Maganti M, Armstrong S et al. Initial results of the chordal-cutting operation for ischemic mitral regurgitation. J Thorac Cardiovasc Surg, 2007;133:1483-1492.

12. Masuyama S, Marui A, Shimamoto T, Nonaka M, Tsukiji M, Watanabe N et al. Chordal translocation for ischemic mitral regurgitation may ameliorate tethering of the posterior and anterior mitral leaflets. J Thorac Cardiovasc Surg, 2008;136:868-875.

13. Rama A, Praschker L, Barreda E, Gandjbakhch I. Papillary muscle approximation for functional ischemic mitral regurgitation. Ann Thorac Surg, 2007;84:2130-2131.

14. Ueno T, Sakata R, Iguro Y, Nagata T, Otsuji Y, Tei C. New surgical approach to reduce tethering in ischemic mitral regurgitation by relocation of separate heads of the posterior papillary muscle. Ann Thorac Surg, 2006;81:2324-2325.

15. Hung J, Chaput M, Guerrero JL, Handschumacher MD, Papakostas L, Sullivan S et al. Persistent reduction of ischemic mitral regurgitation by papillary muscle repositioning: structural stabilization of the papillary muscle-ventricular wall complex. Circulation, 2007;116:I259-I263.

16. Hung J, Solis J, Guerrero JL, Braithwaite GJ, Muratoglu OK, Chaput M et al. A novel approach for reducing ischemic mitral regurgitation by injection of a polymer to reverse remodel and reposition displaced papillary muscles. Circulation, 2008;118:S263-S269.

17. Kamohara K, Banbury M, Calabro A, Popovic ZB, Darr A, Ootaki Y et al. A novel technique for functional mitral regurgitation therapy: mitral annular remodeling. Heart Surg Forum, 2006;9:E888-E892.

18. Fukamachi K, Popovic ZB, Inoue M, Doi K, Schenk S, Ootaki Y et al. Changes in mitral annular and left ventricular dimensions and left ventricular pressure-volume relations after off-pump treatment of mitral regurgitation with the Coapsys device. Eur J Cardiothorac Surg, 2004;25:352-357.

19. Messas E, Pouzet B, Touchot B, Guerrero JL, Vlahakes GJ, Desnos M et al. Efficacy of chordal cutting to relieve chronic persistent ischemic mitral regurgitation. Circulation, 2003;108:II111-II115.

20. Bolling SF, Pagani FD, Deeb GM, Bach DS. Intermediate-term outcome of mitral reconstruction in cardiomyopathy. J Thorac Cardiovasc Surg, 1998;115:381-386.

21. Kollar A, Kekesi V, Soos P, Juhasz-Nagy A. Left ventricular external subannular plication: an indirect off-pump mitral annuloplasty method in a canine model. J Thorac Cardiovasc Surg, 2003;126:977-982.

22. Levine RA, Hung J, Otsuji Y, Messas E, Liel-Cohen N, Nathan N et al. Mechanistic insights into functional mitral regurgitation. Curr Cardiol Rep, 2002;4:125-129.

23. Tibayan FA, Rodriguez F, Zasio MK, Bailey L, Liang D, Daughters GT et al. Geometric distortions of the mitral valvular-ventricular complex in chronic ischemic mitral regurgitation. Circulation, 2003;108:II116-II121.